Control No. AP241

HYDRODYNAMIC MODELS OF LAKE ST. CLAIR

by

T.J. Simons and W.M. Schertzer

Aquatic Physics and Systems Division

National Water Research Institute

Burlington, Ontario, Canada L7R 4A6

March 1986

NWRI Contribution #86-10

EXECUTIVE SUMMARY

As part of the 1985/87 Canada-U.S. Upper Great Lakes Connecting Channel Study, it is intended to model material transport and sediment-water exchanges in Lake St. Clair. The first step toward that goal is to model water movements in the lake by numerical methods and to verify the model against extensive current meter observations made during 1985. This is the subject of the present report. In particular, the report provides a very simple and economical procedure for computing circulations in Lake St. Clair as required in many practical applications.

Lake St. Clair is dominated by the hydraulic flow associated with the St. Clair River inflow and the Detroit River outflow. Superimposed on this mean flow is a wind-driven circulation which is highly variable with instantaneous currents comparable to the hydraulic flow. To model this circulation by the usual hydrodynamical methods would be very time-consuming in view of the fact that water-quality studies require water movement computations over extended periods of time. The modelling procedure suggested in this report circumvents this problem by taking advantage of the fact that Lake St. Clair is very shallow with a mean depth around 4 m.

Based on theoretical considerations and experiments with a time-dependent hydrodynamic model of Lake St. Clair, it is shown that the currents adjust themselves to the wind within a period of a few hours. This justifies the use of quasi-steady dynamics for analysis

and simulation of Lake St. Clair circulations when dealing with time scales of a day or longer as done in water quality studies. Using this approach, it is shown that daily-mean currents should be a simple function of the hydraulic flow and the daily wind. The coefficients of this functional relationship are determined in two ways. The first is a least-squares fit to the measured currents (empirical model). The second is the use of a steady-state hydrodynamic model (numerical model). Comparison of results from the empirical model and the numerical model constitutes a novel method of model validation which is found to be preferable over conventional verification methods.

The major conclusions of the study are the following. The empirical model shows that the current directions vary strongly with wind speed due to the associated mixing of the water column but the current speeds tend to increase only slightly with the wind speed. This result appears at first surprising but is explained by recourse to the hydrodynamical model. The speeds of the model current are shown to be proportional to the ratio of wind stress to eddy viscosity. Since the eddy viscosity should increase with wind mixing, the net effect is a rather weak dependence of current speeds on wind stress. By comparing the empirical and numerical model results, a tentative relationship between eddy viscosity and wind stress is arrived at. Lack of information concerning this relationship has been the major impediment to application of hydrodynamical models to shallow lakes. The present study offers a solution which is consistent with theory and supported by observations, yet simple and economical to apply in practical situations.

ABSTRACT

Current measurements made in Lake St. Clair during 1985 are analyzed and compared with results of hydrodynamic models. The analysis is based on daily averaged currents and it is shown that such currents are in quasi-steady balance with the wind. A least-squares fitting procedure is used to decompose measured currents into hydraulic and wind-driven components for different classes of wind mixing. It is found that the current directions vary strongly with mixing but the speeds tend to be less dependent of the wind class.

The numerical model calculations are based on the Ekman theory for finite water depth. It is shown that the speeds of the model currents are proportional to the ratio of wind stress to eddy viscosity. Since the observed current speeds are rather independent of the wind speed, it is concluded that the eddy viscosity increases with the wind stress in a nearly linear fashion. It is found that the directions of the model currents correspond closely with the directions of observed currents. However, the speeds of the hydraulic currents near the bottom are severely underestimated by the model. It is shown that this is due to the no-slip boundary condition at the bottom of the lake and that acceptable simulations of hydraulic flows can be obtained by assuming a more uniform vertical velocity profile.

Based on the data analysis and model verification, a very simple and economic procedure is suggested for computing circulations in Lake St. Clair for extended periods of time as required in many practical applications.

1. INTRODUCTION

The overall objective of this investigation is to model material transport and sediment-water exchanges in Lake St. Clair as part of the 1985/87 Canada-U.S. Upper Great Lakes Connecting Channel Study. The investigation has the following specific objectives:

1. To model water movement in Lake St. Clair by numerical methods and to verify the model against extensive current meter observations made during 1985 (Murthy et al., 1986).
2. To evaluate the various components of the water balance of Lake St. Clair including water level changes due to winds.
3. To model wind-generated waves on Lake St. Clair and to verify the model against wave measurements made in 1985 (Murthy et al., 1986).
4. To model sediment resuspension induced by currents, waves and turbulence and verify the model against measurements made in 1985 (Charlton et al., 1986).
5. To calculate material balances for Lake St. Clair based on water quality surveys and sediment trap sampling during 1985 (Charlton et al., 1986).
6. To use the water movements and sediment resuspension models for calculating transports and sediment-water exchanges of nutrients and contaminants.
7. To merge the above into a comprehensive water quality model of Lake St. Clair.

The present report deals with development and verification of hydrodynamic models of Lake St. Clair. The prime objective is to arrive at a suitable procedure for modelling water transports (objective 1 above). A secondary goal is to model wind-induced water level changes for use in the water balance calculations (objective 2 above). The latter are described in a companion report (Schertzer and Simons, 1986).

2. FIELD MEASUREMENTS

The measurements used for model verification in this study were made during an extensive field program on Lake St. Clair during 1985. A detailed description of the data may be found in the report by Murthy et al. (1986). The present summary will be restricted to the data used for model verification.

Figure 1 shows the locations of wind recorders, current meters and shore-based water level gauges in Lake St. Clair. Nearly all the current meters were placed in two transects of the lake in order to permit a verification of the measurements based on the total water transport through a cross section (Simons et al., 1985). All these current meters were positioned at a depth of 1 m above the bottom. Figure 2 shows the depth variations and current meter moorings along the two transects indicated in Figure 1.

Table 1 presents a summary of available current data for the two transects. The currents were recorded at intervals of 20 minutes. It is seen that the data return is fairly complete for the period June 5 to November 5, 1985, a total of 154 days. Although most current records extend beyond November 5, the period of study is terminated at that time because the wind records do not extend any farther (see following). The currents were decomposed into components along and normal to the transects. The main transect (stations C1-C6) is oriented from SW to NE and the current components along and normal to the transect are counted positive to the NE and NW, respectively. The current components along and normal to the second transect (stations C7-C9) are taken to be positive to the east and north, respectively.

Figures 3 and 4 present plots of the above defined current components averaged over six hours to eliminate short-term fluctuations due to waves and seiches. The components along the transects are generally negative (in westerly direction) due to the strong hydraulic flow in Lake St. Clair. The largest westward currents are found at Station C1 due to the "funnelling" effect on the flow near the Detroit River. The current components normal to the northern transect are strongly negative (to the south) because about 53% of the St. Clair River flow enters north of this transect (Ibrahim and McCorquodale, 1985). Since the river flow during the period of measurement was about 6300 m^3/s (Schertzer and Simons, 1986), there should be a flow of 3300 m^3/s through the northern transect. Actual interpolation of the measured currents and

integration over the area of the cross section gives a mean value of 3240 m^3/s for the whole period of measurements, which is in excellent agreement with the river flow. The current components normal to the main transect are predominantly negative (to the SE) for stations C3-C6 and positive (to the NW) for station C1. It will be shown in the following that this reflects the curvature of the hydraulic flow which turns south upon leaving the St. Clair River before heading west toward the Detroit River.

Table 2 presents a summary of the wind data available at the time of this study. Winds were recorded at intervals of ten minutes. For the above-mentioned period, June 5 to November 5, 1985, the data return from the first station is nearly complete. Some data gaps appear in the records from stations M2 and M3 but these stations were located side-by-side so that their records could be merged. Fortunately, the data gaps of stations M2 and M3 do not overlap except for a two-day period in October. Because of the central location of these stations, their combined record was used for the computations in this study. The two-day data gap in October was filled in with data from station M1. A picture of the time variation of the wind stress obtained from this wind record may be found in Figure 9 of this report.

3. ELEMENTS OF LAKE CIRCULATIONS

Before entering into the data analysis and model calculations, it is useful to consider the basic elements of hydrodynamic flow in a large lake. Ignoring first any vertical variations of the currents, the vertical mean flow in a lake can be visualized as the combined effect of three processes. The first process is the time-dependent response of the free surface to wind impulses. The currents associated with such seiches are typically uniform over any cross section of the lake and oscillate with the same period as the free surface. Although their instantaneous speeds may be large, these currents become rather insignificant when averaged over periods of a day or so as done in the present study.

The second component of the circulation is caused by sustained wind forcing in the presence of depth variations. For most large lakes these topographic currents account for nearly all the water movements and they apper as closed circulation cells moving around the basin in a counterclockwise direction. However, in a shallow lake such as Lake St. Clair, the bottom friction is too large for topographic wave propagation and hence the topographic circulation will take the form of the steady-state response to wind. This means that currents in the nearshore zone tend to flow in the same direction as the wind while currents in the open lake will run against the wind. For a discussion of these circulations, reference is made to Simons (1980, ch. 5).

The third component of the circulation is that associated with inflowing and outflowing rivers. While this hydraulic circulation is negligible in most large lakes, it is a major component of the circulation in Lake St. Clair. The inflow into Lake St. Clair is almost completely accounted for by the St. Clair River while the only outflow is that of the Detroit River. Since these river flows are fairly constant in time, the resulting hydraulic circulation may be taken to be quasi-steady.

Superimposed on the above vertical-mean circulation is a vertical current profile which depends on surface and bottom stresses and the vertical eddy viscosity. The general properties of this current profile are known from the familiar Ekman theory (for a review see Simons, 1980, ch. 3). According to this theory, the surface water tends to flow to the right of the wind and the bottom current deviates to the left of a pressure-driven current such as the hydraulic flow. The detailed solution depends on the local water depth and the vertical eddy viscosity which, in turn, depends on the wind mixing. Since the currents in the 1985 field study on Lake St. Clair were measured at a depth of 1 m above the bottom, allowance must be made for deviations of these currents from the vertical mean flow.

The present study will concentrate on daily-averaged circulations. First, water level changes and the associated currents will be computed with a time-dependent model. These seiche currents are relatively small when averaged over a day but, for completeness, the observed current may be corrected for the seiche components. The

remainder of the measured currents will then be analyzed under the assumption that, on a time scale of a day or longer, the circulations are in approximate steady-state balance with the forcing. This assumption will be justified by estimating the frictional time scale for Lake St. Clair which indicates that the currents adjust themselves to the forcing within a period of a few hours. This will be confirmed by results from the time-dependent model.

4. WIND SET UP AND SEICHE CURRENTS

This section deals with wind-induced variations of the surface level and the associated currents. The results will be used to estimate lake levels from shore-based measurements in the water balance calculations (Schertzer and Simons, 1986) and to correct observed currents for the seiche components before analyzing the flow for time scales of a day or longer. The procedure is to compute water levels with a hydrodynamic model and to compare the results with observations at shore locations (see Figure 1). If the model predicts the right water levels, it may be assumed that the model also produces a good estimate of the components of the currents which accompany the seiche activity of the lake.

The model is a conventional storm surge model. The basic equations are the linearized vertically-integrated equations of motion and the continuity equation

$$\frac{\partial U}{\partial t} = - gH \frac{\partial h}{\partial x} + fV - BU + \frac{\tau_x}{\rho} \qquad (1)$$

$$\frac{\partial U}{\partial t} = - gH \frac{\partial h}{\partial y} + fU - BV + \frac{\tau_y}{\rho} \qquad (2)$$

$$\frac{\partial h}{\partial t} = - \frac{\partial U}{\partial x} - \frac{\partial V}{\partial y} \qquad (3)$$

where U, V are the components of the vertically-integrated current in x,y direction, h is the free surface displacement, H is the local water depth, g is gravity, f the Coriolis parameter, ρ is density, τ_x, τ_y the wind stress components and B a depth-dependent bottom drag coefficient. Based on model studies of the Great Lakes (Simons, 1980, 1985; Schwab, 1983), B is estimated as

$$B = 5 \times 10^{-3} H^{-2} \qquad (4)$$

where H is expressed in meters and B has units of s^{-1}.

The equations are solved on a rectangular Richardson lattice. Thus, the variables are staggered in space with the surface elevation being computed at the centre of a grid square and the components of the current vector normal to the sides of the square. Spatial derivatives are approximated by central differences and the Coriolis term is obtained by averaging over four surrounding points. Time extrapolation proceeds by using a single-step forward scheme for each variable in turn, thereby using the most recent values of the two

other variables. Due to the structure of the equations, this procedure is equivalent to a forward-backward scheme for the Coriolis terms and a leapfrog scheme for the pressure-divergence terms. The timestep is determined by the grid spacing and the depth of the lake. For a discussion of the numerical procedure, reference is made to Simons (1980, ch. 4).

The numerical grid used for Lake St. Clair has a mesh size of 1 km, thus covering the lake by approximately 1100 grid squares (Figure 5). The maximum depth during the 1985 field season was 9.5 m which sets an upper limit of 73 seconds for the time step of the free-surface model. The mean depth during the field season was 4.3 m. The corresponding free surface wave travels with a speed of 23.5 km/hr and the length scale of the lake is 40 km which should give a basic seiche period of about 3.5 hours.

Since the lake is so shallow, the frictional damping according to (4) is very large. For the mean depth of 4.3 m the bottom drag coefficient B becomes equal to 2.7×10^{-4} s^{-1}. The inverse of this value is the time required for the current to decrease by a factor e. This follows from Eq. (1) by ignoring all terms on the right except for the bottom friction, thus

$$\frac{\partial U}{\partial t} = - BU \qquad (5)$$

the solution of which is

$$U = U_0 e^{-Bt} \qquad (6)$$

where U_0 is the initial current. Therefore, the current decreases by a factor e over a period of time equal to B^{-1} = 3700 sec ≈ 1 hour. This is a fraction of the basic seiche period and hence the seiches in Lake St. Clair must be strongly damped.

To illustrate these properties of the lake, Figure 6 presents the total water transport through the main cross section of the lake (Figure 1) as computed by the free-surface model for two cases of wind forcing. In each case, the wind stress is suddenly applied and has a constant value of 0.1 Nm^{-2}. In the first case (solid line), the wind blows normal to the cross section toward the NW while in the second case (dashed line) the stress direction is along the cross section toward the NE. The rapid damping of the seiches implies that the mean circulation for periods of a day and longer may be computed from steady-state models. This is the theoretical basis for the procedures used in the remainder of this study.

The time-dependent model was run for the period June 5 - November 5, 1985, using wind observations at the centre of the lake (Figure 1). The wind stress was obtained from the square of the wind speed with a drag coefficient ranging from 1.5 x 10^{-3} for speeds less than 10 m s^{-1} to 3.0 x 10^{-3} for speeds over 20 m s^{-1} with a linear variation in between (Simons, 1985). To verify the model, hourly values of the computed water level differences (setup) between

stations L1 and L2 of Figure 1 were compared with the observed setup, a total of 3,696 values. The correlation coefficient was 0.84 but the slope of the linear regression of computed and observed setup was too small. In order to adjust the slope of the maximum likelihood estimate to unity, the computed results must be multiplied by a factor 1.8. Figure 7 shows the resulting plot of computed versus observed setup. The long-term mean value of the observed setup is 2.85 cm.

The adjustment of the computed results in the above manner is one of the procedures to estimate effective wind drag coefficients over water (Simons, 1975). In the present case, this procedure would indicate that the drag coefficient used in the model should be increased by as much as 80% which is not inconsistent with earlier studies of this type (Simons, 1980). However, allowance should be made for the fact that the model computes water levels at a distance of half a grid spacing away from the shore. If it is assumed that the depth decreases linearly from this point to the shore, then the additional surface elevation at the shore, h', may be estimated from the formula presented by Simons (1975):

$$h' = a \ln \left(\frac{H_0 - a}{h' - a} \right) \qquad a = \frac{1.5 \tau_s}{\rho g \beta} \tag{7}$$

where H_0 is the water depth half a grid spacing (0.5 km) away from the shore, β is the bottom slope and the other symbols have the same meaning as in (1). For the grid squares adjacent to L1 and L2

(Figure 1), the values of H_0 are 1.8 and 2.4 m, respectively, and hence the bottom slope would be about 4×10^{-3}. For a wind stress of 0.1 Nm^{-2} the value of a would then be 0.4 cm and h' = 2 cm. For comparison, the steady-state setup between L1 and L2 computed from the numerical model for a NE stress of 0.1 Nm^{-2} is 4 cm (see Figure 6). This suggests that the nearshore setup may add as much as 50% to the setup computed by the model. This correction decreases somewhat for higher stress values but it may be assumed to explain about half of the 80% increase of computed water levels which was required above to obtain agreement with observations. If the remaining adjustment is to be made up by increasing the wind-stress coefficient, then it follows that all solutions of the model should be multiplied by 1.4. This is done in the following when the model currents are used.

5. STEADY-STATE THEORY

The foregoing considerations justify the use of quasi-steady dynamics for analysis of Lake St. Clair circulations for time scales of a day or longer. To start off, a brief summary will be presented of the theory of steady-state circulations known as Ekman theory. The basic assumption of the Ekman theory is that the vertical eddy viscosity is known. The vertical profile of the current can then be expressed in terms of the local pressure gradient (surface slope) and the wind stress. The solutions depend on the nondimensional ratio ε as follows.

$$\varepsilon \equiv \frac{H}{D} \qquad D \equiv \pi \sqrt{\frac{2\nu}{f}} \tag{8}$$

where H is the water depth, ν the kinematic vertical eddy viscosity ($m^2\ s^{-1}$), f the Coriolis parameter (s^{-1}) and D has the same units as the water depth and is known as the Ekman depth.

The eddy viscosity in a lake such as Lake St. Clair is thought to be of order $10^{-3}\ m^2\ s^{-1}$ while $f = 10^{-4}\ s^{-1}$. A typical Ekman depth is then 14 m, about three times as large as the typical water depth of Lake St. Clair, hence $\varepsilon = 0.3$. For such shallow water the Ekman solutions resemble steady-state currents in the absence of rotation which, according to (8), is equivalent to infinite Ekman depths. Therefore, the basic character of the solutions for Lake St. Clair can be illustrated by solutions for the case of no rotation.

In the absence of rotation, the vertical profile of the current, u, is related to the pressure gradient, dp/dx, and the wind stress, τ, as follows

$$u = \frac{1}{\rho\nu}\left[(Z + H)\,\tau + \frac{1}{2}\,(Z^2 - H^2)\,\frac{dp}{dx}\right] \tag{9}$$

where Z is the vertical coordinate measured upward from the mean surface level and the other symbols have been defined before. Vertical integration of the current between the bottom and the surface gives

$$U = \frac{1}{\rho\nu}\left[\frac{1}{2}H^2\,\tau - \frac{1}{3}H^3\,\frac{dp}{dx}\right] \tag{10}$$

If the latter is integrated over a complete transect of the lake, the result is the total water transport across that transect. In the absence of rivers, the steady-state transport across any section must vanish and hence the pressure gradient caused by the wind is equal to

$$\frac{dp}{dx} = \frac{3}{2}\left(\overline{H^2}/\overline{H^3}\right)\tau \tag{11}$$

where the bar denotes a mean over the cross section. This is the conventional formula for the steady-state surface slope induced by wind. Substituting this into (9), one finds the following solution for the wind-driven current in a very shallow lake.

$$u = \frac{\tau}{\rho\nu}\left[Z + H + \frac{3}{4}\left(\overline{H^2}/\overline{H^3}\right)\left(Z^2 - H^2\right)\right] \tag{12}$$

which means that the current measured at a given location should be proportional to the ratio of wind stress to eddy viscosity. This theoretical result is of crucial significance for the following data analysis. Since the eddy viscosity represents a form of vertical mixing, its value may be expected to increase with wind stress. If this increase is more or less linear, then the speed of the wind-driven current should be rather independent of the wind speed according to (12). The physical explanation is that an increase of

wind at constant eddy viscosity will lead to a corresponding magnification of the vertical current profile. However, a simultaneous increase of the eddy viscosity will reduce the vertical shear of the profile and hence offset the first effect. Conversely, it may be concluded that, if observed current speeds appear rather independent of the wind speed, then the eddy viscosity is proportional to the wind stress. It will be shown that this is suggested by the current meter observations in Lake St. Clair.

It should be pointed out that, although Lake St. Clair is shallow enough for the Ekman solutions to resemble those for the case of no rotation, effects of rotation cannot be completely ignored. This may be illustrated by graphical presentations of the shallow water Ekman solutions summarized, for example, by Simons (1980). The solutions selected here are those for pressure-driven currents without wind such as the hydraulic flow associated with rivers flowing into and out of a lake. Figure 8 shows relationships between the vertical-mean flow and the current 1 m above the bottom as a function of vertical eddy viscosity and water depth. The upper half of the figure shows the ratio of the vertical-mean current to the bottom current while the lower half presents the clockwise turning from the bottom current to the vertical-mean current. Note that the solutions toward the right side of the figure approach the pressure-gradient part of the no-rotation solution (9) because effects of rotation decrease with increasing eddy viscosity. These no-rotation solutions are shown by dashed lines in the upper half of Figure 8.

6. EMPIRICAL MODEL

The measured currents at stations C_1 - C_6 on the main transect of Lake St. Clair (Figure 1) will now be interpreted with reference to the steady-state theory of lake circulations. As seen in the foregoing, this theory should be applicable to Lake St. Clair for time scales of a day or longer and, hence, this study will deal with daily-averaged currents and forcing. It is assumed that the dynamics of the circulation are essentially linear so the current is a simple superposition of the flow induced by the two components of the wind stress, τ_x, τ_y, and the hydraulic flow. It is also assumed that the wind stress is uniform over the lake. Let $v_0(x,y\ z)$ be the hydraulic component of the current at a given location (x,y) and depth (z), $v_1(x,y,z)$ the current component induced in the same point by a unit wind stress in x-direction and $v_2(x,y,z)$ the current due to a unit wind stress in y-direction. The total current at point (x,y,z) can then be written

$$v = v_0 + \tau_x v_1 + \tau_y v_2 \qquad (13)$$

The wind-stress components can be written as

$$\tau_x = \tau \cos \theta, \qquad \tau_y = -\tau \sin \theta \qquad (14)$$

where τ is the magnitude of the stress and θ an angle measured clockwise from the orientation of the x-axis. As noted earlier, when dealing with the main transect of Lake St. Clair (Figure 1), the x-axis lies on the transect pointing to the NE and the y-axis is normal to the transect toward the NW, but the orientation of the coordinate system is, of course, arbitrary. Substitution of (14) into (13) results into

$$v = v_0 + \tau (v_1 \cos \theta - v_2 \sin \theta) \tag{15}$$

or also

$$v = v_0 + \tau A \sin (\theta + \alpha) \tag{16}$$

where

$$A = (v_1^2 + v_2^2)^{1/2} \qquad tg\alpha = -v_1/v_2 \tag{17}$$

Given the series of daily-mean values of measured currents, v, and wind stress, τ_x, τ_y, the coefficients v_0, v_1, v_2 of Eq. (13) can be determined by a least-squares fit. Clearly, if the theory above is applicable, the least-squares fit should have the form of Eq. (16). According to the theory outlined before, the coefficients depend on the vertical eddy viscosity which, in turn, depends on the wind mixing. The daily-mean wind stress may be inadequate to estimate this

mixing since it does not differentiate between strong oscillatory winds and weak constant winds with the same daily-mean stress. A better indicator of wind mixing is the daily rms (root-mean-square) value of the stress which will be denoted by $\hat{\tau}$. Using this parameter, the data will be divided into different classes of wind mixing and the least-squares fitting procedure will be applied to each class separately. These empirical results will then be compared with results from numerical models. This verification method appears more instructive than comparing individual current measurements with model results.

According to Eq. (12) the wind-driven current should, theoretically, be proportional to the ratio of wind stress to eddy viscosity. Hence, the empirical model coefficients v_1 and v_2 defined by (13) and the corresponding amplitude A defined by (17) would be proportional to the inverse of the vertical eddy viscosity. If, furthermore, the eddy viscosity would increase linearly with wind stress, then the empirical model coefficients would become inversely proportional to the stress and (15) - (16) could be written

$$v = v_0 + v_1' \cos\theta - v_2' \sin\theta \qquad (18)$$

$$v = v_0 + A' \sin(\theta + \alpha) \qquad (19)$$

where the new model coefficients denoted by primes are independent of the wind speed. Conversely, if a least squares fit of (18) - (19) to

the measured currents produces the same estimates of the coefficients for different classes of winds, then the eddy viscosity must be proportional to the wind stress.

The first step of the empirical modelling procedure (13) - (19) is to separate the data into classes of wind mixing based on the daily rms values of the stress, $\hat{\tau}$. Various classes have been considered in this study and all of them produced consistent results. The classes selected for discussion here are the following:

$$\begin{aligned} &\text{Class 1:} && \hat{\tau} < .45 \\ &\text{Class 2:} && .45 \leq \hat{\tau} < .90 \qquad (10^{-1}\ \mathrm{Nm}^{-2}) \\ &\text{Class 3:} && \hat{\tau} \leq .90 \end{aligned} \tag{20}$$

In some cases the first and second classes will be subdivided into two classes as follows:

$$\begin{aligned} &\text{Class 1a:} && \hat{\tau} < .30 \\ &\text{Class 1b:} && .30 \leq \hat{\tau} < .45 \qquad (10^{-1}\ \mathrm{Nm}^{-2}) \\ &\text{Class 2a:} && .45 \leq \tau < .60 \\ &\text{Class 2b:} && .60 \leq \tau < .90 \end{aligned} \tag{21}$$

This results in roughly the same number of days for each of the four subdivisions.

7. WATER TRANSPORT THROUGH MAIN TRANSECT

Before applying the empirical model to observations at given locations, it will be used to analyze the total water transport through the main cross section of Lake St. Clair (Figure 1). The

advantage of the transport calculations is that the observations can be checked for mass conservation (Simons, 1985). For instance, in case of steady-state wind-driven circulations, the total transport through any cross secion of a closed lake must vanish. On the other hand, the hydraulic transport must be consistent with the distribution of inflows and outflows. On the basis of averages compiled by Ibrahim and McCorquodale (1985), it is estimated that 8% of the St. Clair River is discharged into area 1 of Figure 1. Since the mean flow during the period of interest is about 6300 m^3/s (Schertzer and Simons, 1986), there should be a positive (northwestward) flow of 500 m^3/s through the main cross section of Lake St. Clair, independent of wind direction.

Figure 9 presents time series of daily-mean wind stress components, daily rms values of the stress and daily-mean transports through the main transect of Lake St. Clair (Figure 1). The wind stress components are oriented along and normal to the transect, that is, toward the NE and NW, respectively, and the water transport is counted positive to the NW. The transport is obtained by multiplying the NW-components of the measured currents by the local depth, interpolating the results by an objective interpolation scheme and integrating over the cross section. The result may be corrected for the seiche component of the flow by recourse to the solution of the free-surface model discussed before. This solution is presented at the bottom of Figure 9. As anticipated, this correction is so small that it may be ignored.

Table 3 presents results of the least-squares fitting procedure for the period June 5 - November 5, 1985. The third and fourth column show average values of the daily-mean resultant wind stress and the daily rms value of the stress for each class. The next three columns present the results of fitting model Eqs. (15) - (17) while the last three columns were obtained by fitting Eqs. (18) - (19). The mean value V_0 represents the flow component which is independent of the wind, i.e. the hydraulic flow. This part of the solution should be the same for both empirical models. This is seen to be generally true. The same holds for the phase angle α. The most interesting result is that the amplitude of the wind-driven flow estimated from (18) - (19) is more or less independent of the wind class. Note also that this amplitude A' is approximately equal to the amplitude A, obtained from (15) - (17), multiplied by the mean stress for the wind class (τ). Recalling the discussion of Eqs (18) - (19), it may be concluded that the eddy viscosity increases with wind stress in a quasi-linear fashion.

Figure 10 illustrates some results of the empirical model fit according to Eqs. (18) - (19). The dashed lines represent the hydraulic flow, V_0, while the solid curves show the wind-driven transport. The hydraulic flow as well as the phase shift of the wind-driven flow show a pronounced dependence on the wind class. In order to explain this, it must be recalled that the currents were measured at a depth of 1 m above the bottom. According to the steady-state Ekman theory (Figure 8), this current should deviate to

the left from the vertical-mean flow such that the angle of deviation decreases with eddy viscosity. Since it was found that the eddy viscosity increases with wind stress, the smallest angles of deviation should be found for the highest wind class. Indeed, Table 3 shows that for that case the phase angle α approaches zero which means that the bottom current runs against the wind, i.e. the pressure gradient or surface setup approaches the no-rotation result given by Eq. (11). Similarly, Table 3 shows that with increasing wind the hydraulic flow estimated from the bottom currents gets closer to the hydraulic transport corresponding to the river flows (500 m^3/s, positive). For weak winds, the bottom currents deviate to the left and, since the hydraulic flow is predominantly to the SW, the estimated hydraulic transport across the main transect is strongly negative.

The foregoing discussion shows that the empirical model result agrees with steady-state theory in a qualitative sense. In order to obtain a more quantitative comparison, steady-state circulations in Lake St. Clair may be computed by numerical models. The model used in this study solves the shallow-water Ekman equations on a rectangular grid with a grid spacing of 1 km. For a discussion of the numerical procedure, the reader is referred to Simons (1980, ch. 5). A model of this type computes in each grid point the steady-state mean flow and the vertical profile of the current for a given wind stress and a given eddy viscosity. For comparison with the observations, the transport across the main transect of Lake St. Clair was computed from

the model by multiplying the solution at a depth of 1 m above the bottom by the depth in each grid point on the transect and then integrating over the transect. The model transport computed in this fashion should not be confused with the actual transport based on the vertical-mean flow computed by the model. The latter is independent of the winds and equal to the imposed hydraulic flow across the transect (500 m^3/s, positive).

For a range of values of the vertical eddy viscosity, the numerical model computed the hydraulic flow, the flow induced by a unit wind stress along the x-axis (along the transect) and the flow caused by a unit wind stress along the y-axis (normal to the transect). These solutions correspond, of course, with the coefficients v_0, v_1, v_2 of the empirical model (13) - (15) and hence the wind-driven transport can be expressed in terms of amplitude and phase in accordance with (16) - (17). The model transports across the main section of the lake (as computed from the solutions 1 m above the bottom) are plotted against the eddy viscosity in Figure 11. The dashed curve in the upper part of Figure 11 is proportional to the inverse of the eddy viscosity. It is seen that the amplitude dependence on eddy viscosity closely approximates the simple solution (12).

The black dots and open circles in Figure 11 are the results of the empirical model (Table 3) plotted against the average value of the daily rms wind stress, $\hat{\tau}$, for each wind class. The black dots represent the main wind classes defined by Eq. (20), the open circles

show the subdivisions of the first two classes, Eq. (21). As seen from the horizontal scale at the bottom, it has been tentatively assumed that the eddy viscosity (m^2/s) is about $0.02\ \hat{\tau}$ (N/m^2). This produces good agreement between numerical and empirical model results for the amplitude of the wind-driven transport and the same proportionality is suggested by the phase angle. However, the hydraulic flow suggests that the eddy viscosity should be considerably smaller or that the bottom current is underestimated by the no-slip boundary condition applied at the bottom in the Ekman model used here. As seen in Figure 8, the resulting current speed at 1 m above the bottom is typically only half as large as the vertical-mean speed. With a more appropriate boundary-layer approximation, the vertical profile becomes much more uniform. This would mean that the model-computed hydraulic transport could become twice as large and, hence, of the same magnitude as the empirical model results. Evidence in support of this hypothesis will be provided in the following.

8. CURRENTS AT INDIVIDUAL STATIONS

The empirical model given by Eqs. (13) - (19) will now be applied to the two components of the currents measured in individual stations and the results will be compared with numerical model solutions. According to Eq. (15) the components of the current may be written as

$$u = u_0 + \tau (u_1 \cos \theta - u_2 \sin \theta)$$
$$v = v_0 + \tau (v_1 \cos \theta - v_2 \sin \theta) \qquad (22)$$

while the model corresponding to Eq. (18) is

$$u = u_0 + u_1^1 \cos \theta - u_2^1 \sin \theta$$
$$v = v_0 + v_1^1 \cos \theta - v_2^1 \sin \theta \qquad (23)$$

where the subscript 0 refers to the hydraulic flow, the subscript 1 to the current induced by a wind stress along the main transect (to the NE) and the subscript 2 to the flow caused by a stress normal to the main transect (to the NW). The angle θ is measured clockwise from the orientation of the main transect, i.e. from the NE.

As before, the empirical model solutions $(u_0, u_1, u_2, v_0, v_1, v_2)$ are determined by a least-squares fit between series of daily-mean observed currents and wind stress. Using daily rms values of the stress $(\hat{\tau})$ as an indicator of vertical mixing, the data will be subdivided into the classes given by Eq. (20). The numerical model solutions will be obtained from the shallow water Ekman model with a grid mesh of 1 km for different values of the vertical eddy viscosity. The model comparison will employ graphical presentations of the vectors (u_0, v_0), (u_1, v_1), (u_2, v_2). Note that this verificaiton method compresses the data and model results into a few diagrams and therefore is much more efficient than conventional verification techniques.

Figure 12 presents the hydraulic currents and the currents induced by a unit wind stress (10^{-1} Nm^{-2}) along and normal to the main transect of Lake St. Clair (Figure 1) as obtained from the empirical model (22) for the three classes of wind mixing given by Eq. (20). The speed of the hydraulic current is independent of mixing but the bottom current deviates to the left from the vertical-mean flow such that the angle is greatest for weak mixing in agreement with Figure 8. This explains the apparent negative hydraulic transport (to the SE) across the main transect when the observed bottom currents are multiplied by the depth and integrated over the cross section (Table 3).

The speed of the wind-driven current appears to decrease with wind mixing but this is a misleading result of the conventional procedure of computing the current response to a unit wind stress (Eq. 22). In actual fact, the mean wind stresses for the three classes of wind mixing are 0.18, 0.45 and 1.09 times the unit stress (see Table 3) and hence the wind-driven currents of Figure 12 are to be multiplied by these values. Alternatively, the currents for the three mixing classes can be obtained by fitting Eq. (23) to the data which leads to essentially the same results (see Table 4). Thus, the actual current is found to increase with wind speed at most stations. However, it is important to note that the current does not vary in proportion to the stress as would be the case for a linear model with constant eddy viscosity. While the mean wind stress in Table 4 varies by a factor of 6, the mean currents (last column of Table 4) vary by a

factor of 2 only. As explained in the discussion of the total transport across the main transect, the reason is that the eddy viscosity increases with wind mixing and the currents are proportional to the ratio of wind stress to eddy viscosity if the shallow water Ekman theory of Eq. (12) is applicable.

For a quantitative estimate of the relationship between eddy viscosity and wind mixing, the numerical model described above was run for a unit wind stress and a range of values of the eddy viscosity. Since the model is linear, the solutions are proportional to the wind stress and hence the solutions for any wind stress can be obtained immediately. If it is assumed that the eddy viscosity varies approximately in a linear fashion with the rms value of the stress, $\hat{\tau}$ then it follows from the third column of Table 4 that the eddy viscosity for the three mixing classes should vary in the ratio 1:2:4. After some experimentation, it was found that the average currents computed at the measurement locations were comparable to the observed ones if the eddy viscosity for the three mixing classes was given values of 4, 8 and 16×10^{-4} m^2/s. Table 5 presents the model results for a unit wind stress and for the stresses corresponding to the three mixing classes (column 2 of Table 4). The last column of Table 5 compares favourably with the last column of Table 4. Consequently, comparing the values of the eddy viscosity used in the model with the rms values of the stress for the three wind classes, one obtains the relationship

$$\nu = .013 \hat{\tau} \qquad (24)$$

where the eddy viscosity, ν, has units of m^2/s and the wind stress, τ, has units of N/m^2.

Figure 13 presents results from the numerical model for the hydraulic flow and for a unit wind stress along and normal to the main transect for the three values of the eddy viscosity given above. For the hydraulic flow , the directions computed by the model agree with the empirical model result of Figure 12 but the velocities computed by the model are about half as large as the empirical results. As discussed earlier, this discrepancy would disappear if the Ekman solutions illustrated in Figure 8 would be replaced by a current profile with a more or less uniform speed (but not direction) above the measurement depth. Indeed, the vertical-mean current speeds computed by the model agree favourably with the empirical currents. Therefore, it is tentatively concluded that the hydraulic circulation computed by the model is acceptable with respect to the vertical-mean flow and the vertical variation of current directions.

For the wind-driven flow the model solutions show the same general dependence on vertical mixing as the empirical results but the details differ somewhat, in particular for high winds perpendicular to the transect. While the model circulations are independent of the wind speed if Eq. (24) is used (see Table 5), the observed currents

appear to increase with wind speed in some stations (see Table 4). This could suggest that the increase of eddy viscosity with wind speed is somewhat less than linear. However, a more likely explanation is that the no-slip bottom boundary condition used in the present Ekman model is inappropriate. This would mean that the model overestimates the bottom stress and underestimates the currents near the bottom as found earlier for the hydraulic flow. In order to remedy this shortcoming, the effective eddy viscosity of the model might be assigned a value lower than Eq. (24), especially for higher wind speeds. It is therefore tentatively concluded that Eq. (24) gives the upper limit of the eddy viscosity if an Ekman-type model is used for computing wind-driven circulations.

9. CIRCULATION PATTERNS

In conclusion the numerical model will be used to compute steady-state circulation patterns in Lake St. Clair for the hydraulic flow and the wind-driven currents. The solutions will be presented in the form of streamlines of the vertical-mean flow. These streamlines are lines of constant value of the mass transport stream function which is defined as follows

$$U = -\frac{\partial \psi}{\partial y} \qquad V = \frac{\partial \psi}{\partial x} \tag{25}$$

where U and V are the vertically-integrated current components. Thus, the current is inversely proportional to the distance between two adjacent streamlines and the depth. The direction of the current is such that the higher value of the stream function lies on the right. This direction is shown by arrows.

Figure 14 shows the streamlines of the hydraulic flow associated with the inflow of the St. Clair River and the outflow of the Detroit River. The streamlines shown in the figure separate the flows from the North Channel, the Middle Channel, the Southeast Bend of the South Channel and the St. Clair Cutoff. The flow pattern is essentially independent of bottom friction in the range of friction parameters considered in this study. The empirical model currents (see top of Figure 12) have been entered at the locations of the measurement stations. For the higher value of wind mixing, these currents are seen to be aligned with the vertical-mean flow while for lower wind mixing, they deviate to the left. As noted in section 2, interpolation and integration of the measured currents over the northern transect gives a mean value of 3240 m^3/s which is in excellent agreement with the discharge of the North and Middle Channels of the St. Clair River (3300 m^3/s). This supports our earlier conclusion that the vertical profile of the current velocity is nearly uniform above the measurement depth.

Figures 15 and 16 present the results of the Ekman model for winds blowing along and normal to the main transect. The wind stress

is 0.1 N/m^2 and the eddy viscosity is 13.3×10^{-4} m^2/s. Since the model is linear the solutions are proportional to the wind stress. Also, the vertical-mean circulation is found to be nearly proportional to the inverse of the eddy viscosity. Thus, in first approximation, the wind-driven circulation of Lake St. Clair is proportional to the ratio of wind stress to eddy viscosity, just like the simple model of Eqs. (10) - (12). The only difference is that the current directions at different depths depend on the eddy viscosity. For most applications, the vertical-mean circulation is of primary importance. In order to obtain this circulation for arbitrary wind, solutions are first obtained for an arbitrary combination of stress amplitude and eddy viscosity and for two principal wind directions. Next, the actual wind stress is decomposed into the components along the principal axes and each component is multiplied by the corresponding model solution taking into account the ratio of wind stress to eddy viscosity. Since the two principal circulations have to be computed only once and can be saved for future use, this method permits a very economical way of computing daily circulations for a whole season.

Although the foregoing analysis was based on daily averages, the circulations may be computed from the wind stress at time intervals shorter than one day to get a smooth transition from one flow pattern to the next. In that case the distinction between the rms value of the stress ($\hat{\tau}$) and the resultant stress (τ) becomes less important. Then, if the eddy viscosity is taken to increase linearly with the stress in accordance with Eq. (24), the wind-driven solution

becomes independent of the wind speed and is completely determined by the wind direction. Thus, the circulations shown in Figures 15 and 16 are applicable to all wind speeds as long as the ratio of eddy viscosity to wind stress remains the same. For instance, based on 1985 wind observations, a typical stress value would be τ=.06 N/m^2 (see Table 3), the corresponding eddy viscosity would be ν = 8x10^{-4} m^2/s, and the wind-driven circulations would look like Figures 15 and 16.

The patterns of the wind-driven circulation are in agreement with simple models of topographic circulations. If the wind is aligned with the main transect of Lake St. Clair (Figure 15), the currents are relatively weak since the depth variation normal to the transect is rather small. The current meters placed along the transect are all located in the broad band of relatively weak return flow. On the other hand, if the wind blows normal to the transect, the depth-induced circulation is stronger and runs with the wind at the nearshore stations and against the wind in the central stations. These wind-driven currents are large enough to significantly alter the underlying pattern of the hydraulic circulation.

ACKNOWLEDGEMENTS

The field program was carried out by J.A. Bull, F.M. Boyce and C.R. Murthy. Discussions with A. El-Shaarawi and P.F. Hamblin clarified many aspects of the analysis.

REFERENCES

Charlton, M., et al., 1986: Water quality surveys and sediment trap measurements in Lake St. Clair during 1985 (to be published).

Ibrahim, K.A. and J.A. McCorquodale, 1985. Finite element circulation model for Lake St. Clair. J. Great Lakes Res. 11, 208-222.

Murthy, C.R., et al., 1986: Physical measurements in Lake St. Clair during 1985 (to be published).

Schertzer, W.M. and T.J. Simons, 1986: Estimation of the hydrological components of Lake St. Clair. NWRI #86- .

Simons, T.J. 1975: Effective wind stress over the Great Lakes derived from long-term numerical model simulations. Atmosphere, 13, 169-179.

Simons, T.J., 1980: Circulation models of lakes and inland seas. Can. Bull. Fish. Aquat. Sci. 203.

Simons, T.J. 1985: Reliability of circulation models. J. Phys. Oceanogr. 15, 1191-1204.

Simons, T.J., C.R. Murthy and J.E. Campbell, 1985: Winter circulation in Lake Ontario. J. Great Lakes Res. 11, 423-433.

TABLE 1. Current meter data for two transects of Lake St. Clair, 1985. All current meters located 1 m above the bottom.

Station Number	Mooring Number	Sounding Depth(m)	Latitude Longitude	Period of Observation	Period of Missing Data
C9	14	4.37	42.32.41N 82.46.15W	4 Jun 18:20 15 Nov 18:20	
C8	15	4.87	42.32.36N 82.44.57W	4 Jun 17:40 15 Nov 18:40	28 Aug 15:40 9 Sep 16:00
C7	16	5.10	42.32.12N 82.43.44W	4 Jun 17:20 18 Nov 20:00	
C6	17	4.95	42.29.46N 82.38.01W	3 Jun 22:20 18 Nov 16:20	
C5	18	6.82	42.27.27N 82.40.00W	3 Jun 22:00 28 Oct 08:20	11 Jul 16:40 18 Jul 18:00
C4	19	6.66	42.26.10N 82.41.59W	3 Jun 21:20 6 Nov 21:40	
C3	20	6.67	42.24.45N 82.43.56W	9 Jun 16:00 15 Nov 15:40	
C2	21	6.00	42.22.50N 82.45.38W	3 Jun 22:00 1 Oct 20:40	
C1	22	5.57	42.21.19N 82.48.57W	3 Jun 20:00 15 Nov 14:00	

TABLE 2. Wind observations on Lake St. Clair in 1985

Station Number	Mooring Number	Latitude Longitude	Period of Observation	Period of Missing Data
M1	1	42.28.45N 82.48.18W	22 May 15:50 4 Nov 16:40	16 Jun 04:40 27 Jun 13:40
M2	2	42.24.35N 82.42.11W	22 May 17:10 6 Nov 22:10	27 Jun 15:00 8 Aug 16:20 24 Sep 00:80 11 Oct 16:40
M3	3	42.23.57N 82.41.33W	22 May 18:30 6 Nov 23:00	31 May 09:00 12 Jun 17:10 11 Aug 08:50 22 Aug 20:20 9 Oct 21:00 17 Oct 15:30

TABLE 3. Empirical model fit to daily water transport across main transect of Lake St. Clair for different classes of daily rms value of the stress, June 5 - November 5, 1985. Stress units 10^{-1} Nm^{-2}; transport units $10^3 m^3 s^{-1}$; positive to NW; angles in degrees clockwise from NE.

Wind Class	Number of days	Mean Values τ	Mean Values $\hat{\tau}$	Equations (15)-(17) V_0	Equations (15)-(17) A	Equations (15)-(17) α	Equations (18)-(19) V_0	Equations (18)-(19) A^1	Equations (18)-(19) α
τ<.3	39	.12	.19	-1.92	9.6	20	-1.88	1.09	24
.3-.45	37	.25	.36	-1.33	8.6	28	-1.41	2.02	28
τ<.45	76	.18	.28	-1.65	8.9	30	-1.58	1.59	29
.45-.60	33	.40	.53	-1.10	4.5	16	-1.28	1.69	21
.60-.90	28	.54	.72	-.70	3.4	0	- .67	1.75	1
.45-.90	61	.46	.61	-.84	3.9	2	-.84	1.67	4
$\hat{\tau}$>.90	17	1.09	1.26	-.11	1.4	5	0	1.62	1
all $\hat{\tau}$	154	.39	.52	-1.13	2.7	8	-1.11	1.63	16

TABLE 4. Empirical model fit to daily-mean currents for different classes of daily rms value of the stress, June 5 - November 5, 1985. Stess units 10^{-1} Nm^{-2}, model Eqs. (23), solutions for (a) wind along transect and (b) wind normal to transect.

Wind Class	Mean Values τ	Mean Values $\hat{\tau}$	Speed of Wind-Driven Current (cm/s) C1	C2	C3	C4	C5	C6	mean
(a) Wind Along Transect									
$\hat{\tau}$<.45	.18	.28	.4	.8	1.7	2.0	1.8	1.9	1.4
.45-.90	.46	.61	1.4	2.1	2.7	3.1	2.0	2.5	2.3
$\hat{\tau}$>.90	1.09	1.26	.9	2.0	3.2	3.4	1.8	3.0	2.4
(b) Wind Normal to Transect									
$\hat{\tau}$<.45	.18	.28	.8	.9	1.0	1.3	2.1	.9	1.2
.45-.90	.46	.61	.4	1.3	2.0	1.9	2.5	1.8	1.7
$\hat{\tau}$>.90	1.09	1.26	.5	2.0	3.9	4.3	1.8	3.4	2.6

TABLE 5. Computed mean currents 1 m above the bottom at locations of stations C1–C6 for unit stress (.1 N/m^2) and for stresses corresponding to wind classes of Table 4.

Eddy Viscosity (10^{-4} m^2/s)	Wind Stress (10^{-1} N/m^2)	Current (cm/s)	Windstress (10^{-1} N/m^2)	Current (cm/s)
4	1	8.1	.18	1.5
8	1	4.4	.46	2.0
12	1	2.2	1.09	2.4

FIGURE CAPTIONS

Fig. 1 Location of wind recorders, current meters and shore-based water level gauges in Lake St. Clair, June-November, 1985.

Fig. 2 Depth profile and current meter moorings in Lake St. Clair cross sections indicated in Fig. 1.

Fig. 3 Observed current components along the Lake St. Clair transects counted positive to the east for the northern transect (C7-C9) and to the NE for the southern transect (C1-C6).

Fig. 4 Observed current components normal to the Lake St. Clair transects reckoned positive to the north for the northern transect (C7-C9) and to the NW for the southern transect (C1-C6).

Fig. 5 Computational grid of hydrodynamic models of Lake St. Clair.

Fig. 6 Computed NE-ward transport through main cross section of Lake St. Clair (Fig. 1) for step-function wind stress of 0.1 Nm^{-2} toward the NE (solid line) and the NW (dashed line) respectively.

Fig. 7 Computed versus observed hourly water level differences (setup) between stations L1 and L2 (Fig. 1) for June 5 - November 5, 1985.

Fig. 8 Ratio of velocity and difference of direction between vertical mean current and current 1 m above the bottom as obtained from Ekman theory.

Fig. 9 Daily-mean wind-stress components, daily rms values of the stress, daily-mean observed water transport thrugh the main transect of Lake St. Clair and transport computed by free-surface model.

Fig. 10 Empirical model fit to daily values of transport across main transect of Lake St. Clair vs. direction of wind stress for three classes of daily rms value of the stress, June 5 - November 5, 1985.

Fig. 11 Amplitude A and phase α of wind-driven transport and hydraulic transport V_0 as defined by (16). Model results (solid curves) plotted against eddy viscosity, empirical results (Table 3) against "wind mixing" $\hat{\tau}$.

Fig. 12 Hydraulic currents and currents induced by a unit wind stress (10^{-1} Nm^{-2}) along and normal to the main transect of Lake St. Clair as obtained from empirical model (21) for three classes of wind mixing given by (20).

Fig. 13 Same as Fig. 12 but obtained from numerical model for three values of eddy viscosity, ν.

Fig. 14 Computed streamlines (100 m^3/s) of hydraulic flow and corresponding empirical model currents for three classes of wind mixing (see top of Fig. 12).

Fig. 15 Computed streamlines (100 m^3/s) for SW wind and eddy viscosity (m^2/s) equal to .0133 times the wind stress (N/m^2).

Fig. 16 Same as Fig. 15 but for SE wind.

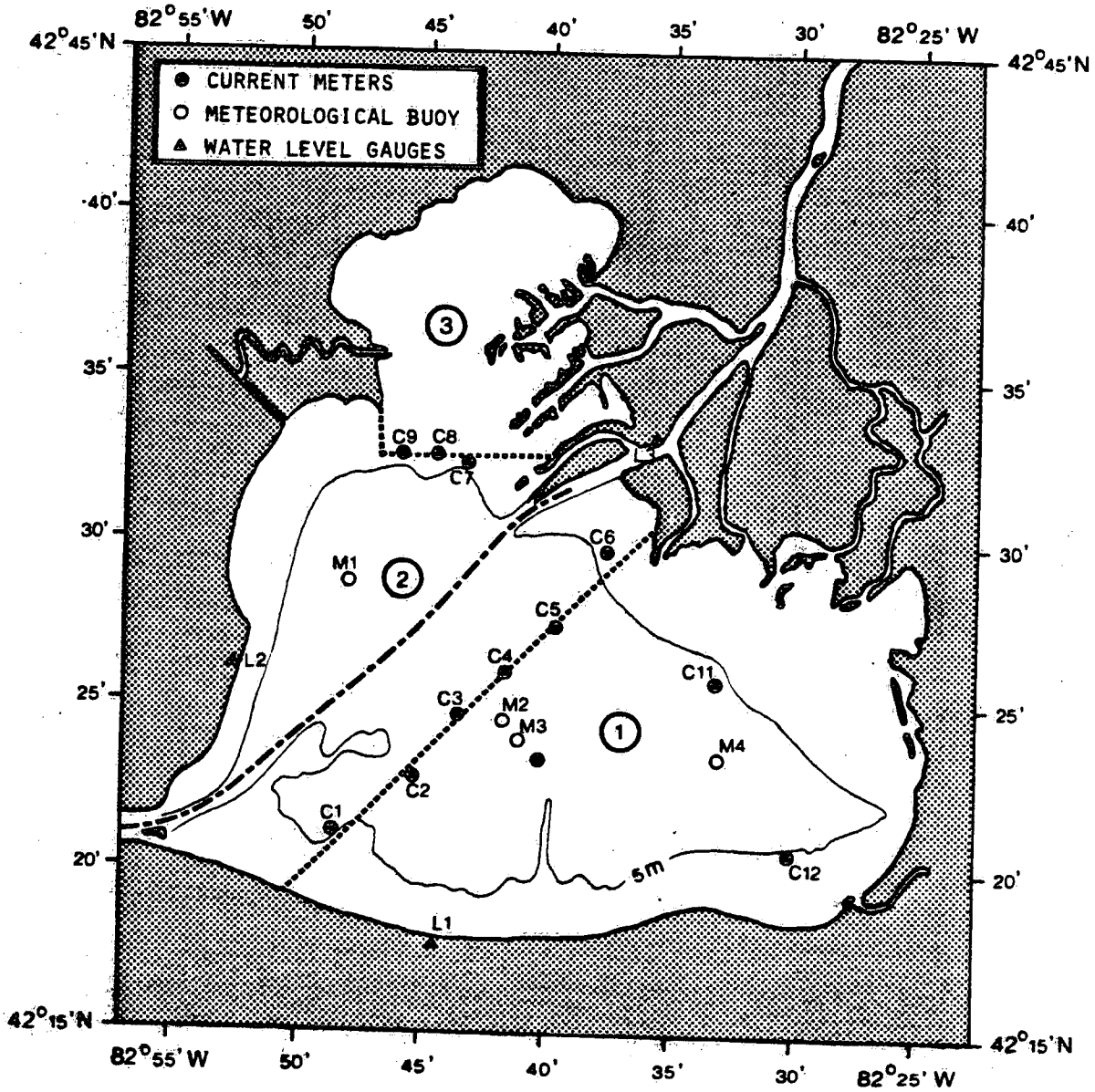
82°55'W
50'
45'
40'
35'
30'
82°25'W
42°45'N
42°15'N
CURRENT METERS
METEOROLOGICAL BUOY
WATER LEVEL GAUGES
40'
35'
30'
25'
20'
C9
C8
C7
C6
C5
C4
C3
C2
C1
C11
C12
M1
M2
M3
M4
L1
L2
5m
1
2
3

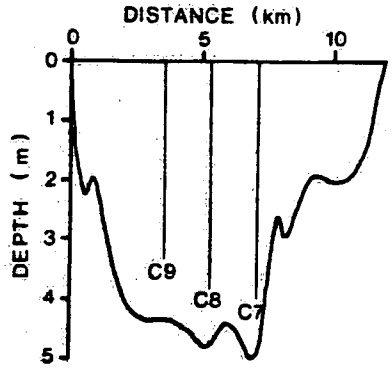
DISTANCE (km)
0
5
10
0
1
2
3
4
5
DEPTH (m)
C9
C8
C7

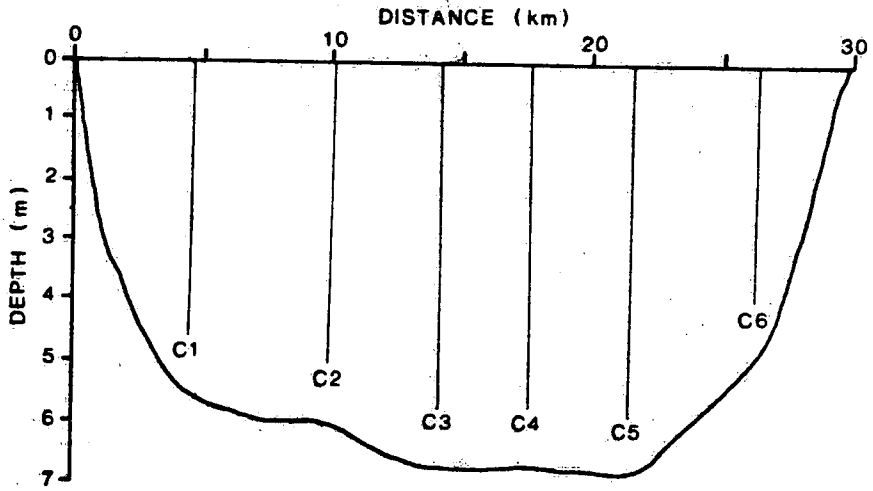
DISTANCE (km)
0
10
20
30
0
1
2
3
4
5
6
7
DEPTH (m)
C1
C2
C3
C4
C5
C6

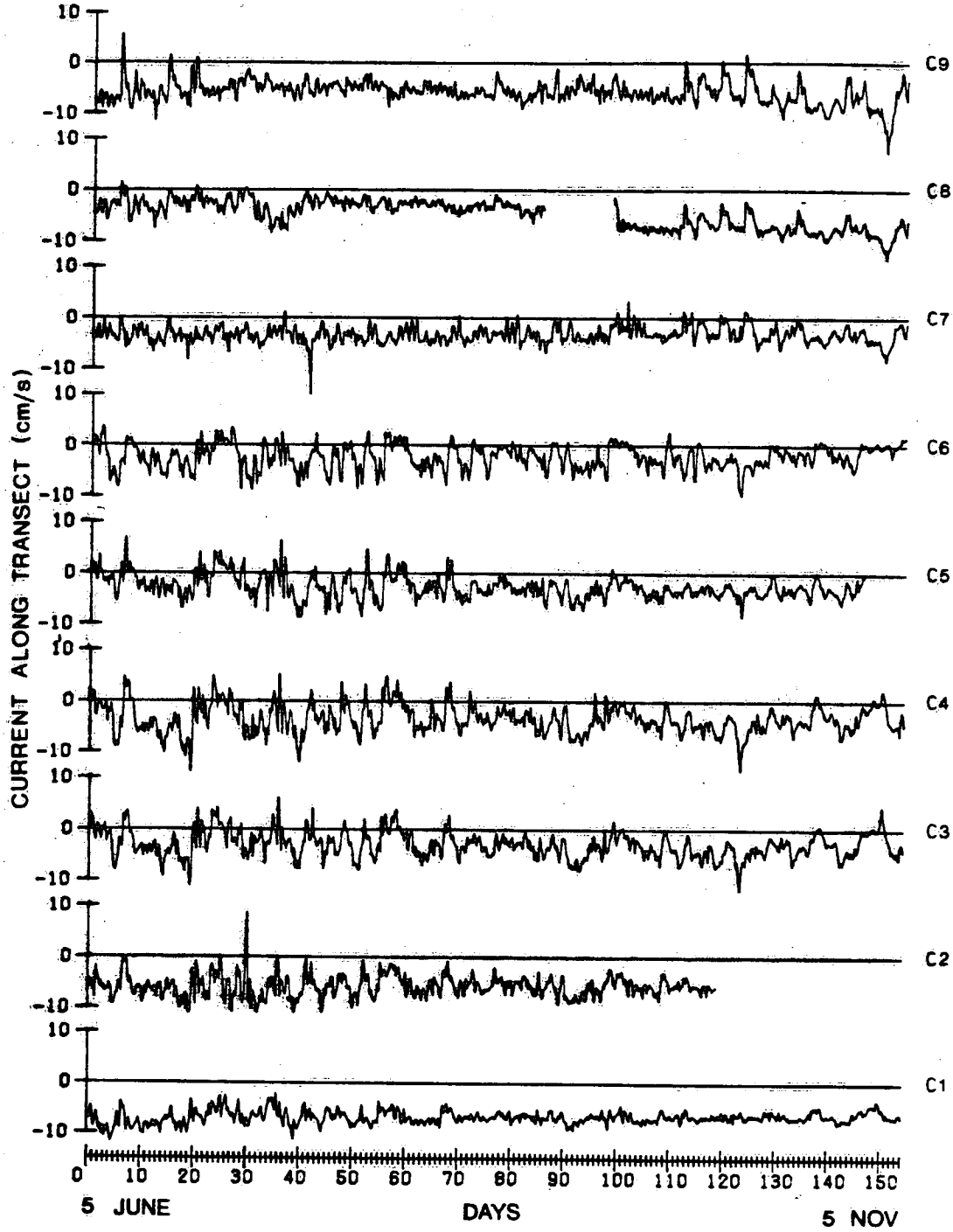
CURRENT ALONG TRANSECT (cm/s)
10
0
-10
C9
C8
C7
C6
C5
C4
C3
C2
C1
0 10 20 30 40 50 60 70 80 90 100 110 120 130 140 150
5 JUNE
DAYS
5 NOV

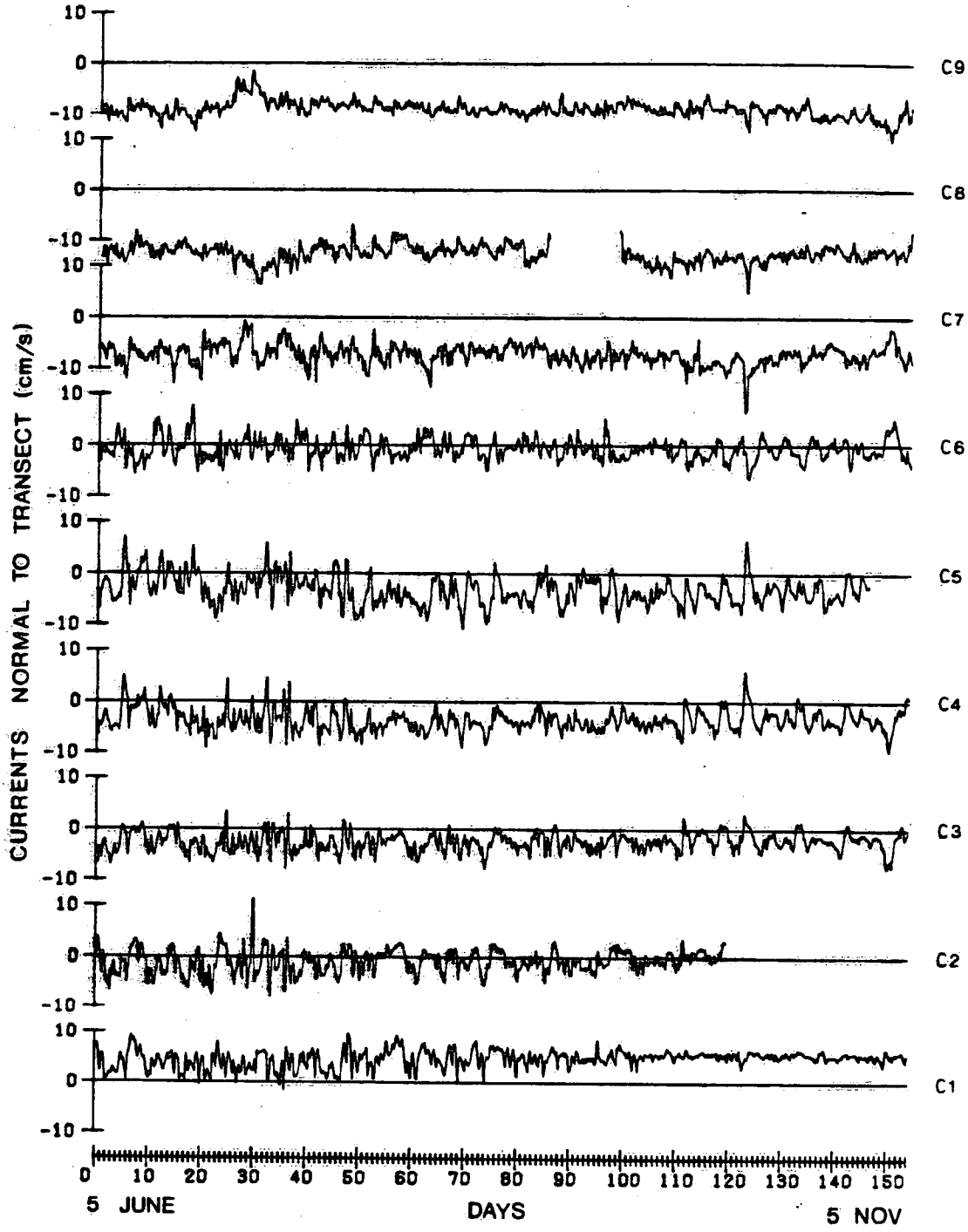
CURRENTS NORMAL TO TRANSECT (cm/s)
10
0
-10
C9
C8
C7
C6
C5
C4
C3
C2
C1
0 10 20 30 40 50 60 70 80 90 100 110 120 130 140 150
5 JUNE
DAYS
5 NOV

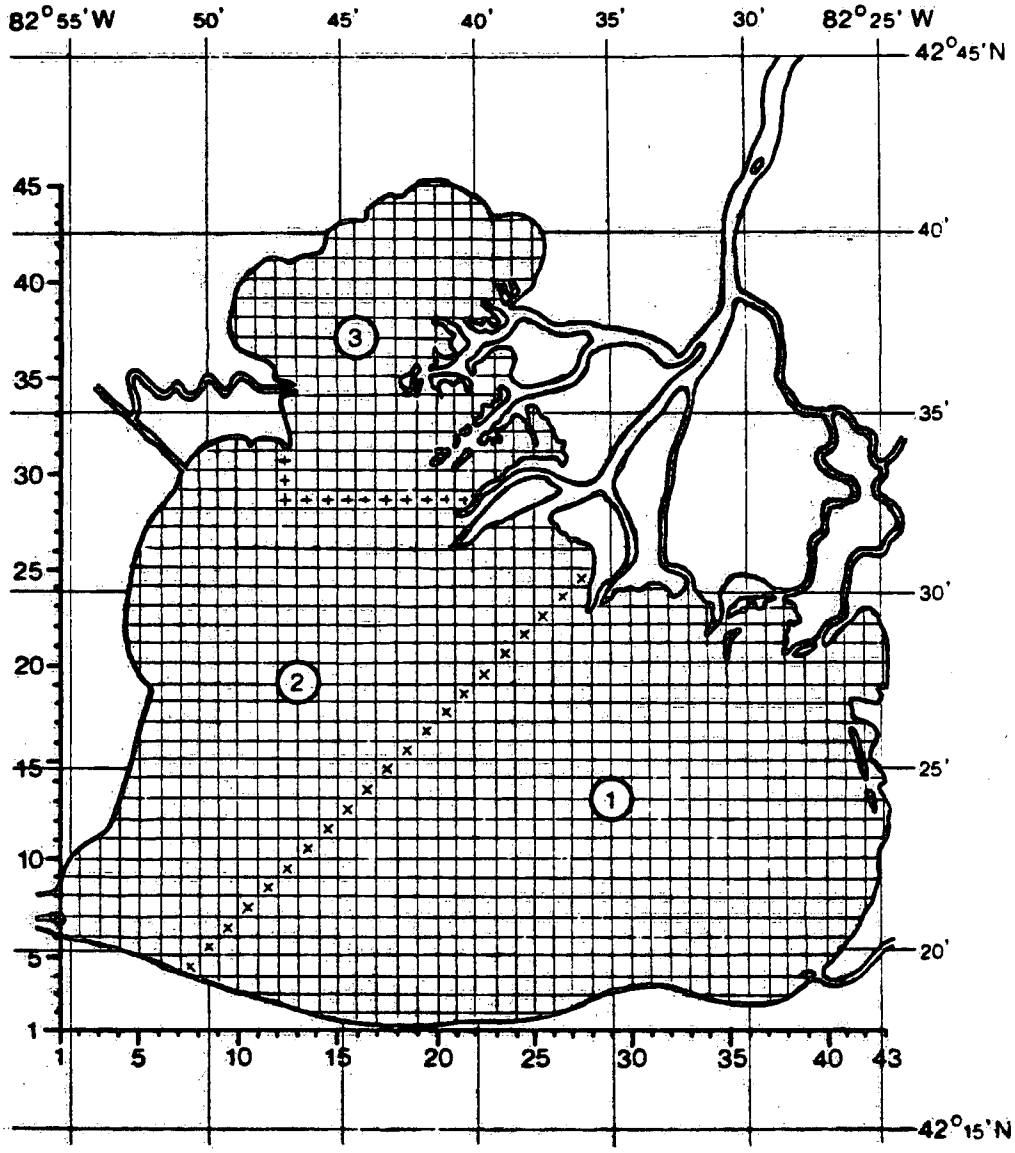
82°55'W
50'
45'
40'
35'
30'
82°25' W
42°45'N
40'
35'
30'
25'
20'
42°15'N
45
40
35
30
25
20
15
10
5
1
1
5
10
15
20
25
30
35
40
43
1
2
3

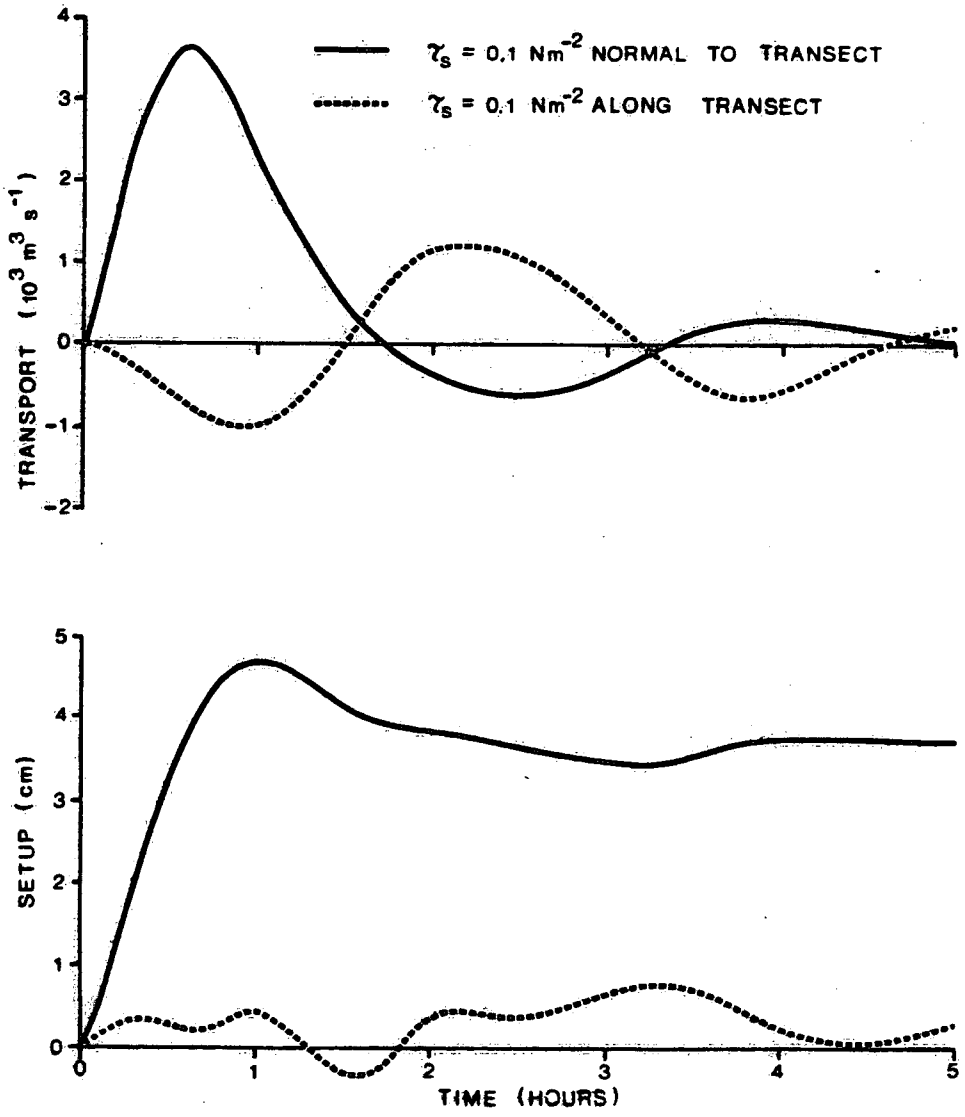
τ_s = 0.1 Nm^{-2} NORMAL TO TRANSECT
τ_s = 0.1 Nm^{-2} ALONG TRANSECT
TRANSPORT (10^3 m^3 s^{-1})
4
3
2
1
0
-1
-2
SETUP (cm)
5
4
3
2
1
0
0
1
2
3
4
5
TIME (HOURS)

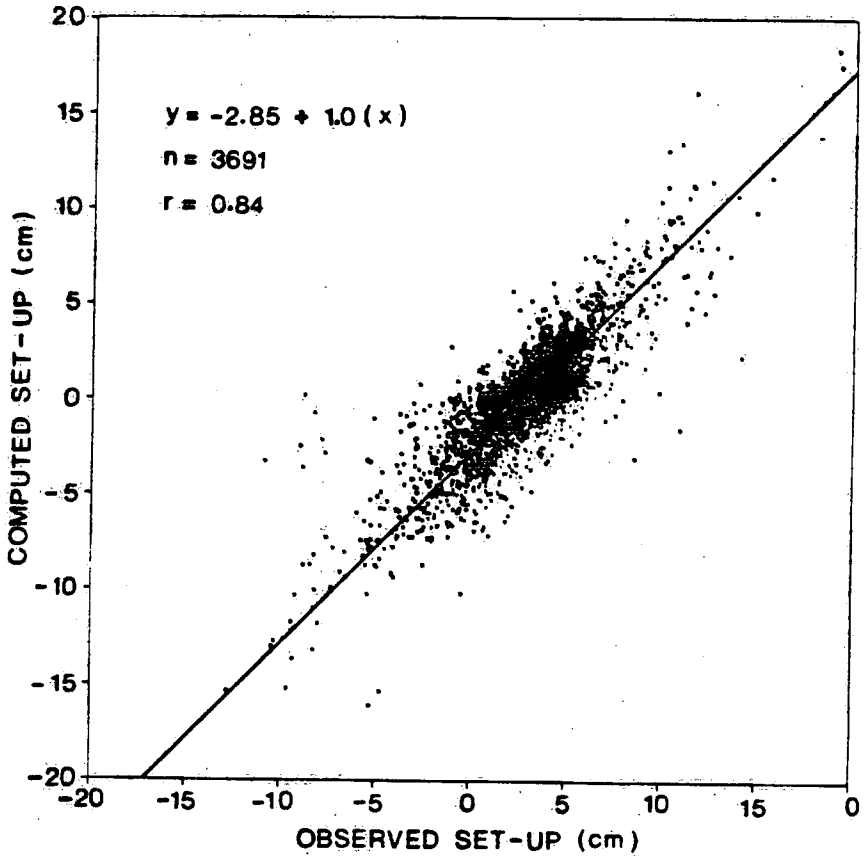
y = -2.85 + 1.0 (x)
n = 3691
r = 0.84
COMPUTED SET-UP (cm)
OBSERVED SET-UP (cm)
20
15
10
5
0
-5
-10
-15
-20
-20
-15
-10
-5
0
5
10
15
0

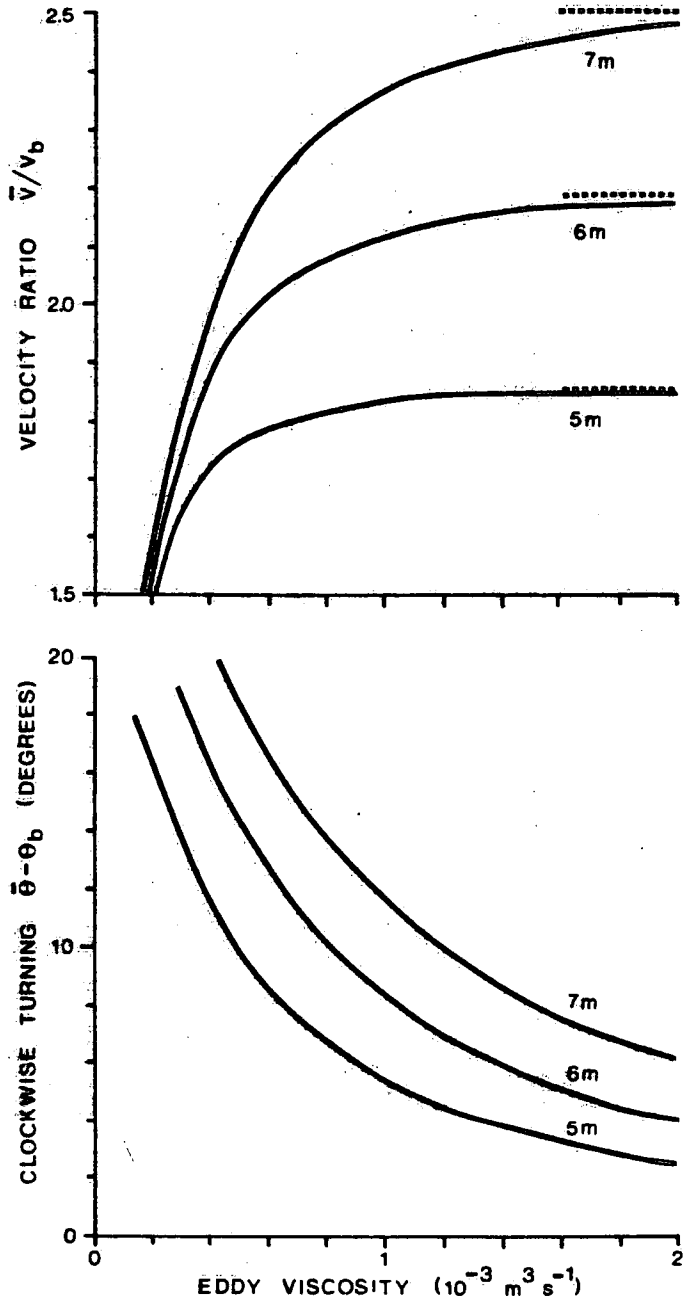
2.5
2.0
1.5
VELOCITY RATIO $\bar{V}/V_b$
7m
6m
5m
20
10
0
CLOCKWISE TURNING $\bar{\theta}-\theta_b$ (DEGREES)
7m
6m
5m
0
1
2
EDDY VISCOSITY (10^{-3} m^3 s^{-1})

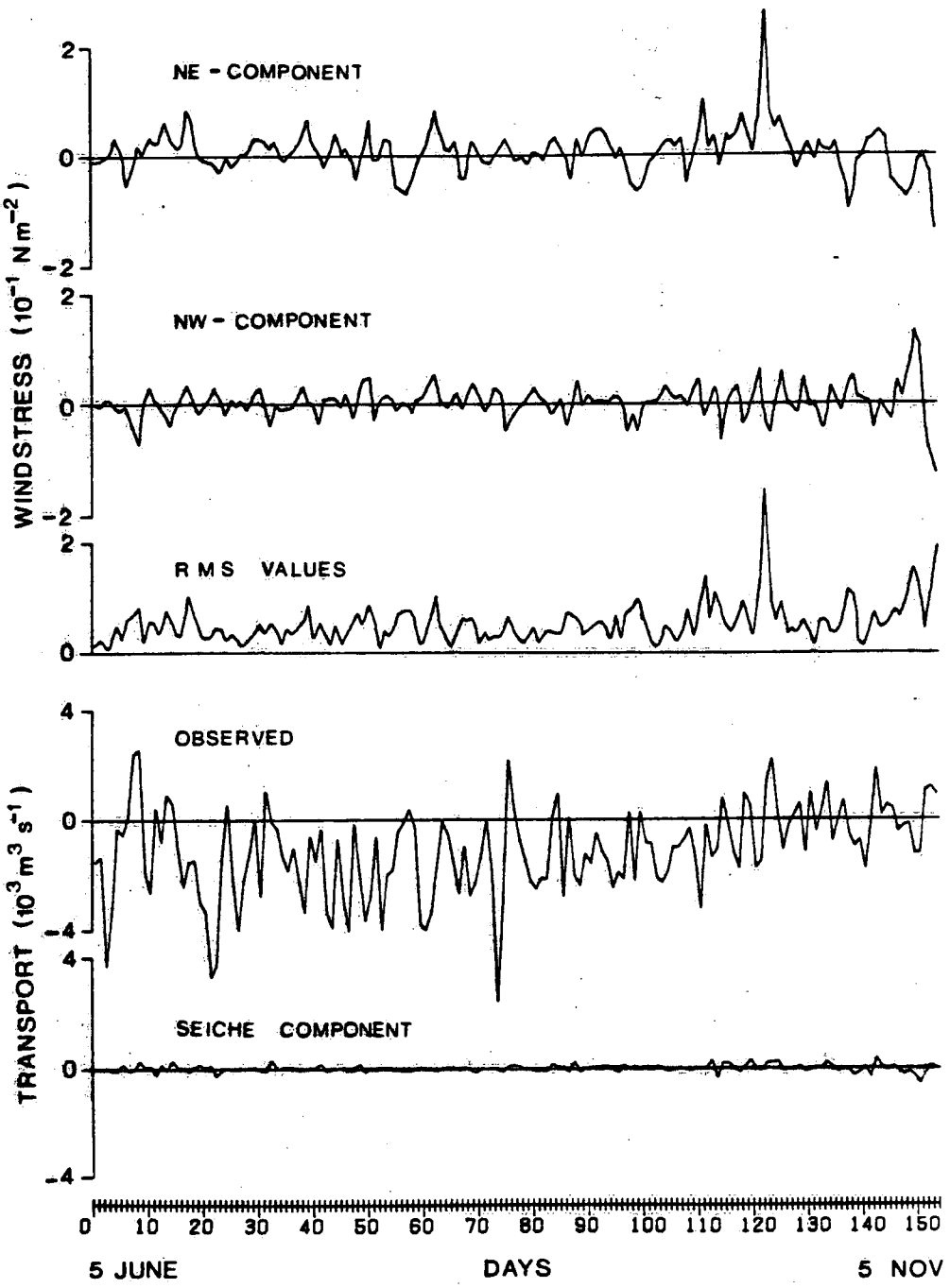
NE - COMPONENT
NW - COMPONENT
RMS VALUES
WINDSTRESS (10^{-1} N m^{-2})
OBSERVED
SEICHE COMPONENT
TRANSPORT (10^{3} m^{3} s^{-1})
2
0
-2
4
-4
0 10 20 30 40 50 60 70 80 90 100 110 120 130 140 150
5 JUNE
DAYS
5 NOV

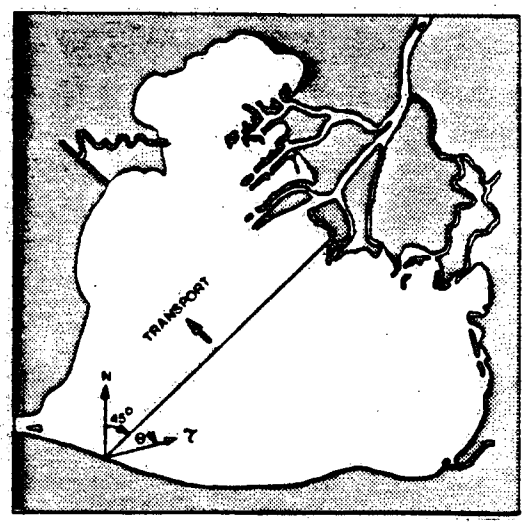

θ = 0° } WIND STRESS ALONG THE CROSS-SECTION
θ = 180° }

θ = 90° } WIND STRESS NORMAL TO THE CROSS-SECTION
θ = 270° }

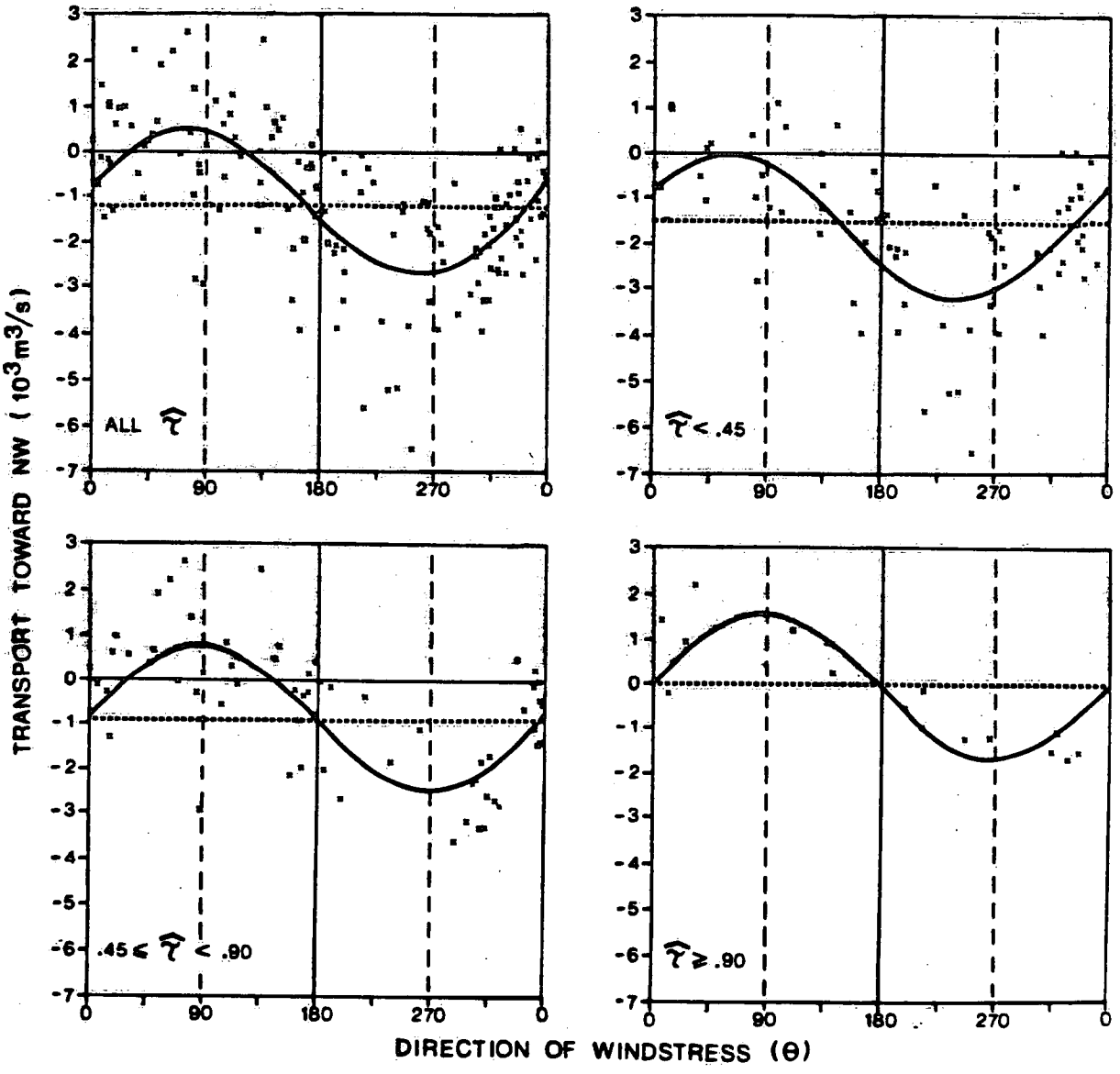

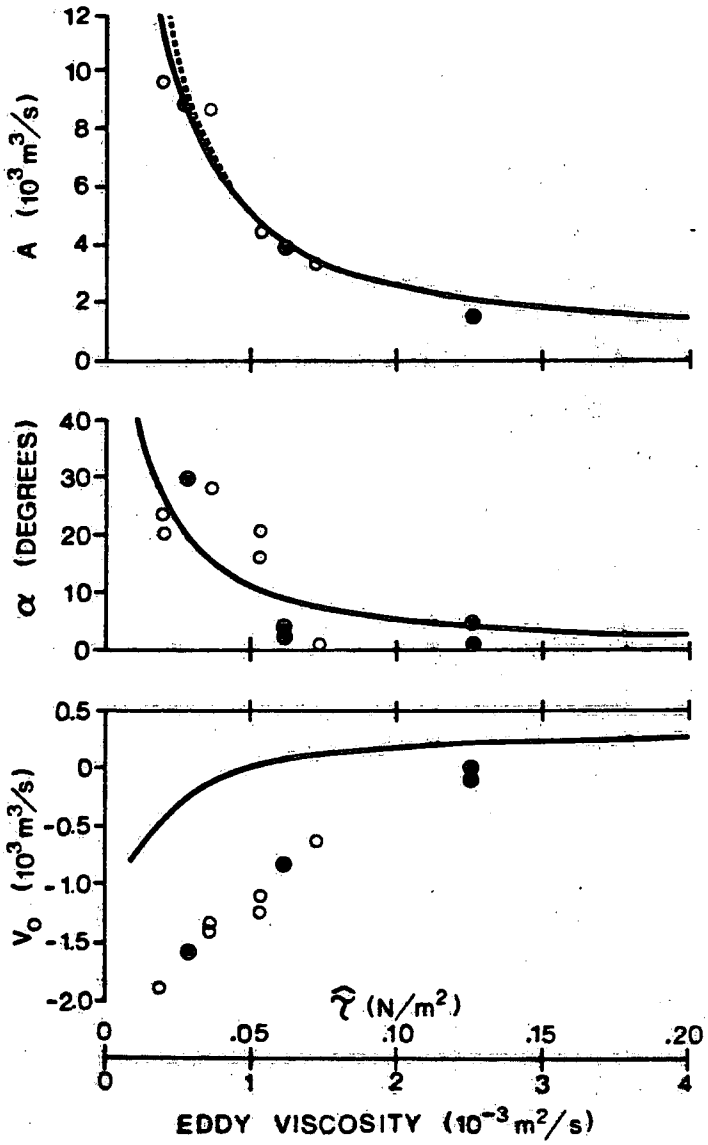
A ($10^3 m^3/s$)
12
10
8
6
4
2
0
α (DEGREES)
40
30
20
10
0
V_o ($10^3 m^3/s$)
0.5
0
-0.5
-1.0
-1.5
-2.0
θ
$\hat{\tau}$ (N/m^2)
0
.05
.10
.15
.20
0
1
2
3
4
EDDY VISCOSITY ($10^{-3} m^2/s$)

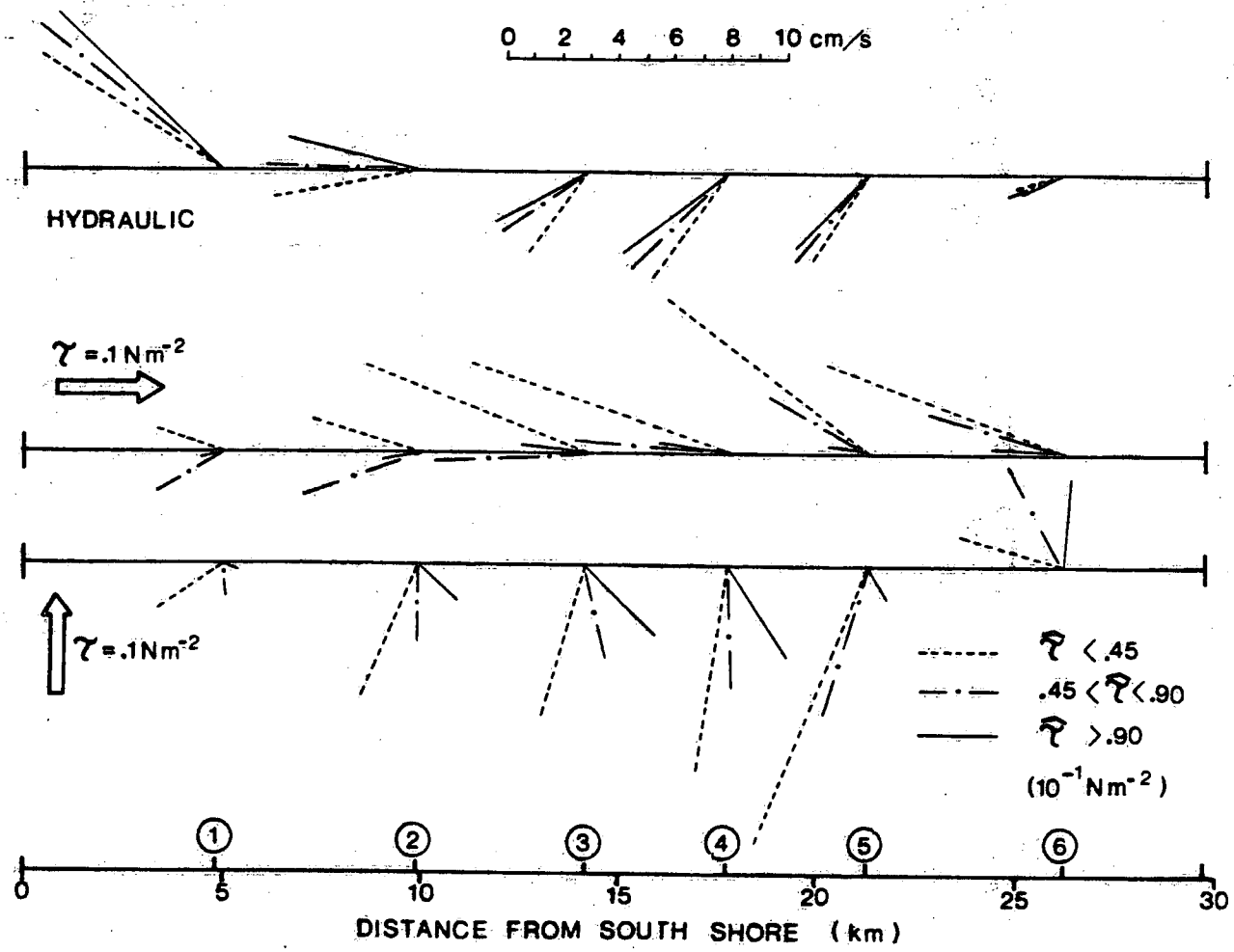
0 2 4 6 8 10 cm/s
HYDRAULIC
τ =.1 Nm⁻²
τ =.1Nm⁻²
τ̃ <.45
.45 <τ̃<.90
τ̃ >.90
(10⁻¹Nm⁻²)
1
2
3
4
5
6
0
5
10
15
20
25
30
DISTANCE FROM SOUTH SHORE (km)

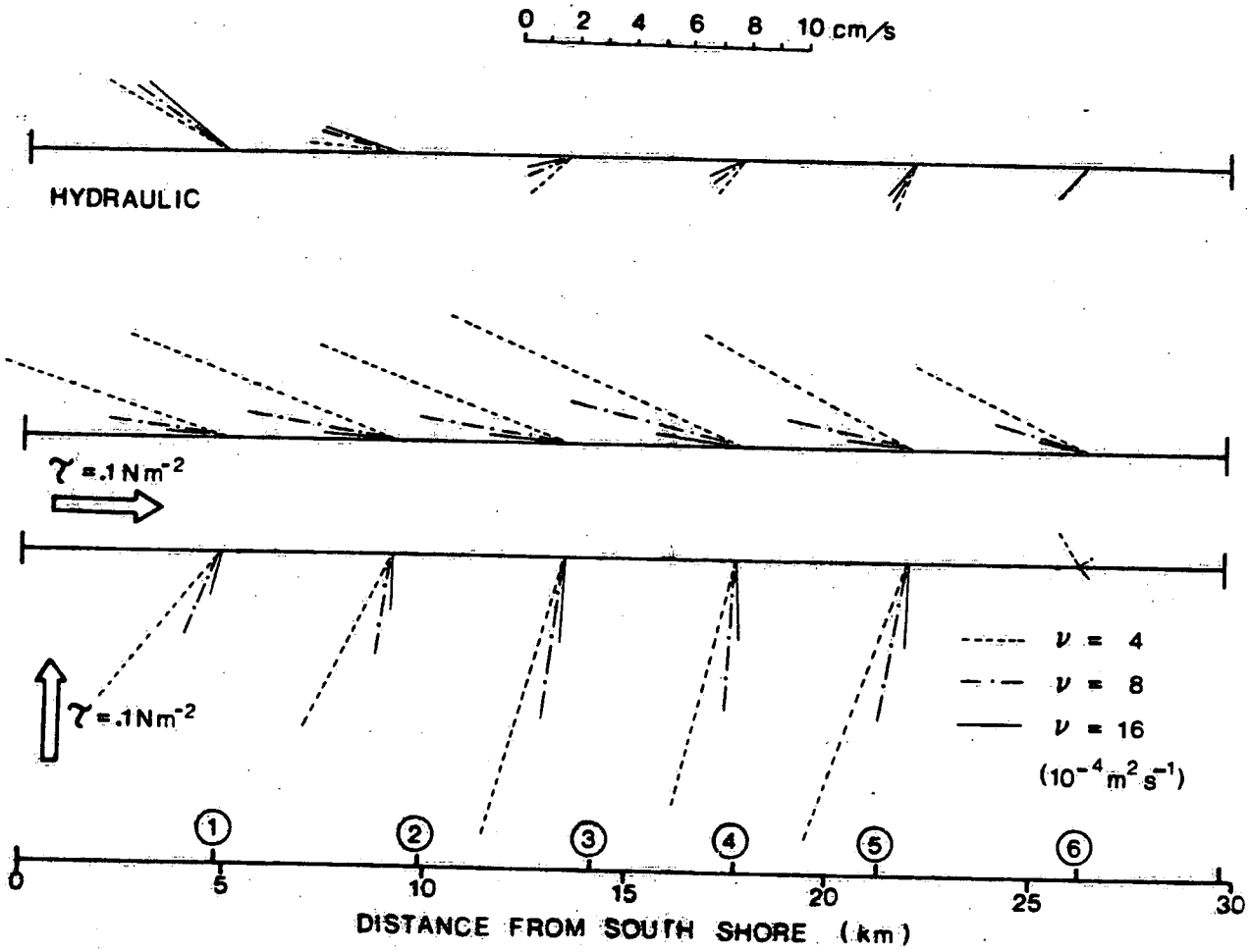
0 2 4 6 8 10 cm/s
HYDRAULIC
τ =.1 Nm⁻²
τ =.1 Nm⁻²
ν = 4
ν = 8
ν = 16
(10⁻⁴ m² s⁻¹)
1
2
3
4
5
6
0
5
10
15
20
25
30
DISTANCE FROM SOUTH SHORE (km)

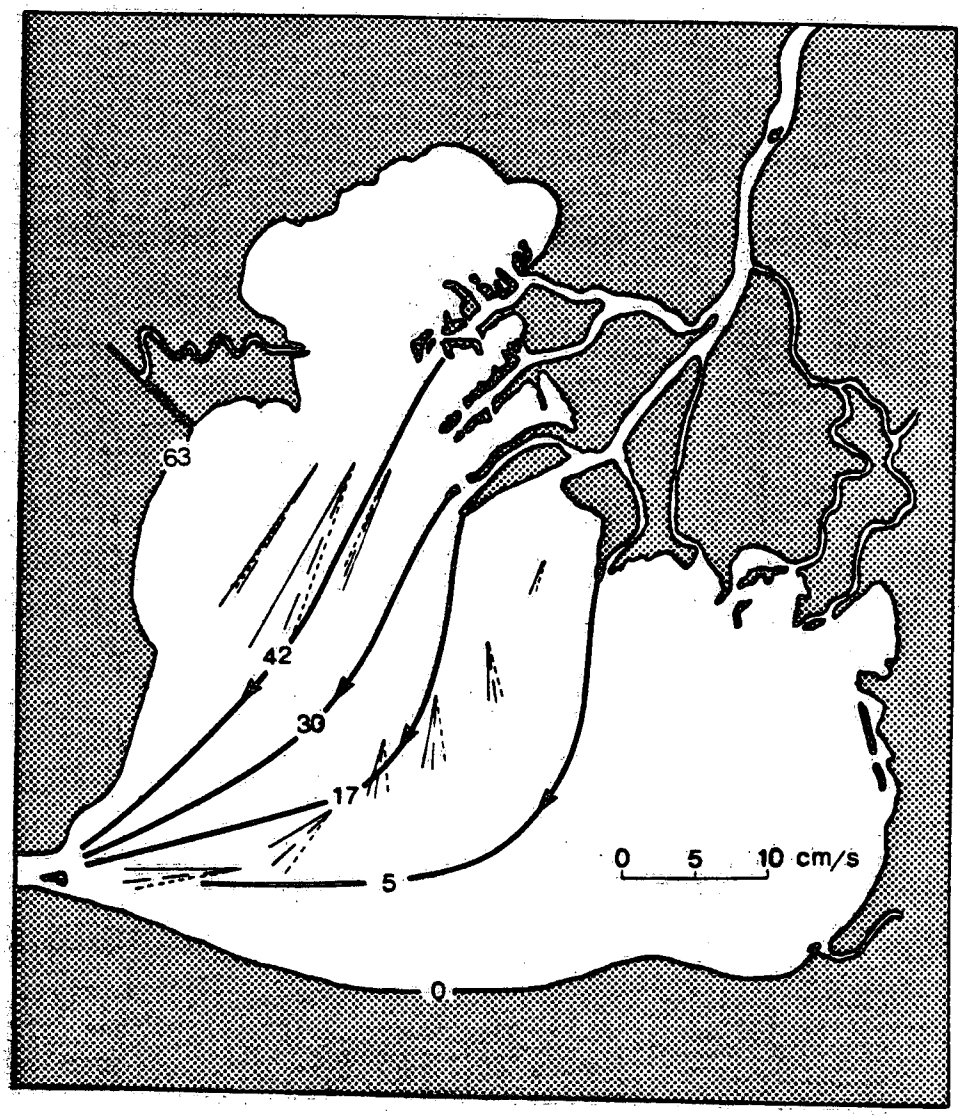
63
42
30
17
5
0
0 5 10 cm/s

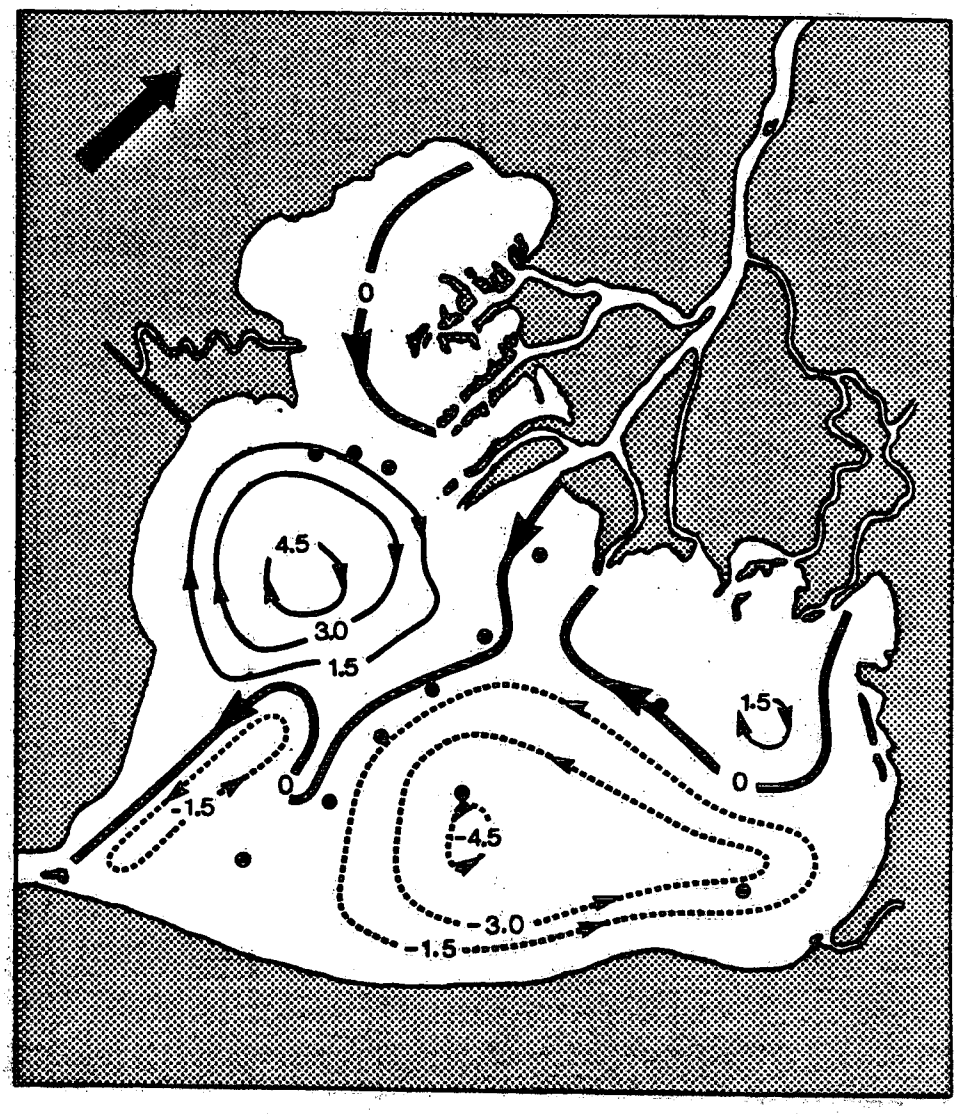
0
4.5
3.0
1.5
0
-1.5
-4.5
-3.0
-1.5
1.5
0

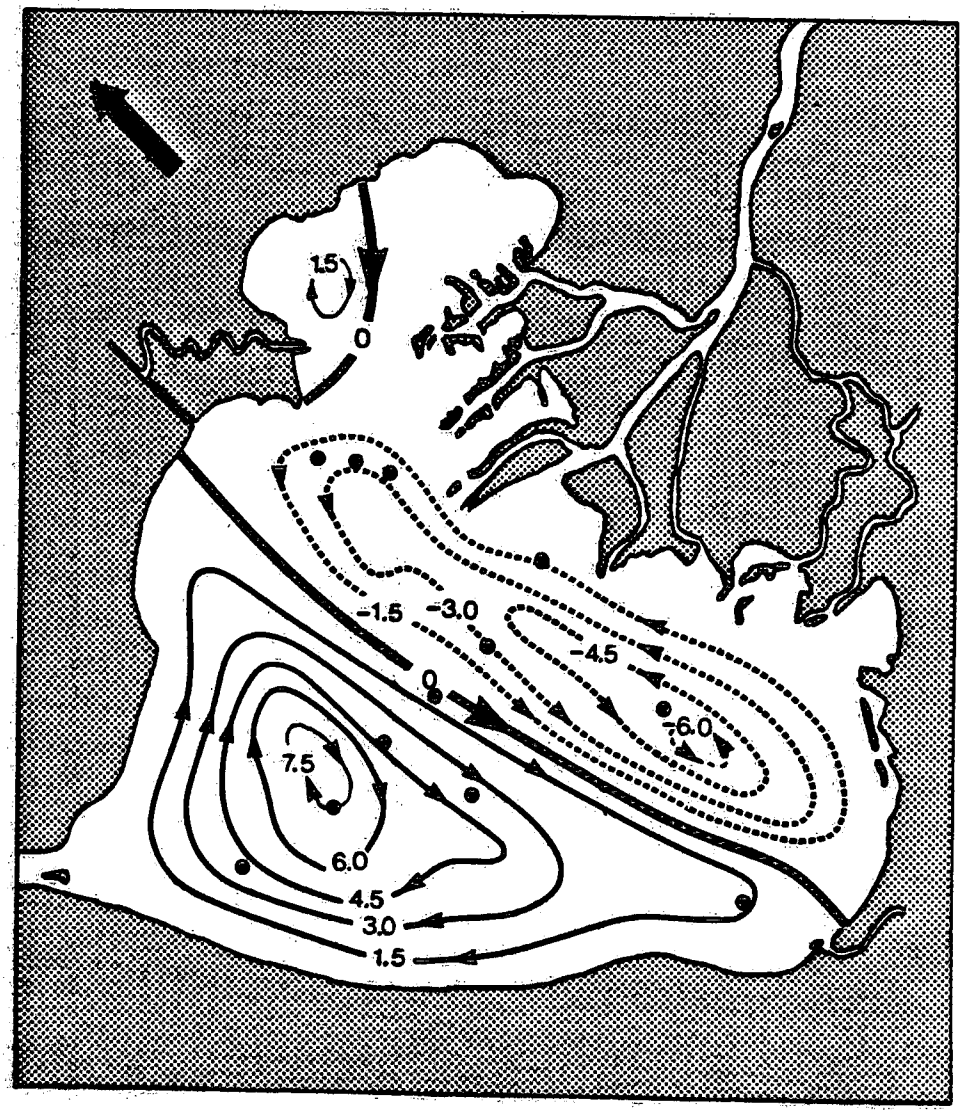
1.5
0
-1.5
-3.0
-4.5
0
-6.0
7.5
6.0
4.5
3.0
1.5